THESIS

APPLICATION OF LARGE-SCALE PARTICLE IMAGE VELOCIMETRY AT THE HYDRAULICS LABORATORY OF COLORADO STATE UNIVERSITY

Submitted by

Kaiwei Chen

Department of Civil and Environmental Engineering

In partial fulfillment of the requirements

For the Degree of Master of Science

Colorado State University

Fort Collins, Colorado

Spring 2018

Master's Committee:

Advisor: Robert Ettema

Christopher Thornton
Peter Nelson
Stuart Lander

ABSTRACT

APPLICATION OF LARGE-SCALE PARTICLE IMAGE VELOCIMETRY AT THE HYDRAULICS LABORATORY OF COLORADO STATE UNIVERSITY

Large-scale particle image velocimetry (LSPIV) is a nonintrusive technique used to measure free-surface velocities of water flow in a manner that produces a two-dimensional vector field of flow velocity. LSPIV is gradually becoming quite widely used as a technique for measuring flow velocities in a range of flow areas. This study used readily available material and devices, and software, to apply LSPIV to flow fields in two laboratory flumes at the Hydraulics Laboratory of Colorado State University; LSPIV had not been used in this laboratory before this study. The applications used pieces of paper as tracer floats in the flow field, and employed a standard iPhone 6s to record video of the tracers moving in the flow field. The video record of tracer movements was then analyzed using Fudaa LSPIV software and Tecplot 360 software to calculate and present the flow velocity data. The applications demonstrated the utility of the LSPIV technique for determining the free-surface flow patterns, and their variations, in experiments done at the Hydraulics Laboratory.

Additionally, this study examined the relationship between the tracer size and LSPIV accuracy with the objective of identifying an optimal width of tracer relative to the width of the flow field and its features. Five sizes of tracer were used in measuring the water-surface flow field through a series of contractions and expansions. It was found that the best tracer size is from about 3.80% to 6.33% of the wide of the channel.

TABLE OF CONTENTS

LIST OF TABLES

LIST OF FIGURES

CHAPTER 1, INTRODUCTION

1.1 Introduction

Large-scale particle image velocimetry (LSPIV) is a nonintrusive technique used to measure instantaneous free-surface velocities, in a manner that produces a two-dimensional vector field of flow velocity. The LSPIV technique was developed from Particle Image Velocimetry (PIV), a quite widely method used for measuring flow velocities in small areas of flow. It was developed for the purpose of providing velocity fields spanning large flow areas in field or laboratory conditions. LSPIV uses floating tracers and a video camera that tracks the temporal displacement of the tracers. It involves the use of a digital image-processing technique, a photogrammetry technique, and a vector analysis technique, and it can be readily applied to flows that do not undergo substantial vertical deformation or aeration. Also, it may involve software to convert velocity vectors into a field of flow pathlines indicating the overall structure of a flow.

This thesis is the first study at Colorado State University (CSU) to apply LSPIV for determining the main water-surface features of flows in experiments. Two flows were studied: flow through a series of contractions and expansions; and, flow around bendway weirs, rock structures used to guide flow in open channels such as alluvial rivers. Also, this thesis investigated the influence of tracer size on the flow velocities determined using the LSPIV method. Prior studies have not addressed this latter aspect of LSPIV use.

1.2 Problem Statement

During the 21st century, efficiency and accuracy are two important considerations as to whether a measurement method should be used. Regarding efficiency, LSPIV can be used at any

location where flow in a channel or river can be observed. Measurements of velocity can be gotten in only a few seconds. Regarding accuracy, LSPIV essentially relies on the performance of digital cameras for acquiring a video of a flow, and on software for analyzing the video so as to produce vectors of flow velocities from several assessments of LSPIV accuracy. Compared to other direct measurements of velocity, typical levels of error are about 3.5% on 1999. Under some severe situations of flow observation, the LSPIC method can still have about a 10% level of error. The LSPIV method is continually being improved to refine its accuracy.

There are several different techniques for measuring flow velocity. Some techniques, such as propeller current meters and acoustic Doppler Velocimeters (ADV), require placing the measuring instrument in the river. However, some river flows do not give easy access for the placing measurement instruments, or are difficult to give whole-field flow measurements, especially unsteady flow situations. Moreover, most other techniques can only calculate the velocity for a single point and are not easy to use or efficient. Some other techniques, such as Particle Image Velocimetry (PIV), can image the velocity fields but cannot be used for large areas of river flow.

The flow fields in many rivers are large, and therefore difficult to measure, especially during change flow conditions. For example, some rivers are 3m wide, some 10 meters wide, and some rivers are 100's of meters in width. Figure 1.1, for example, shows China's Yangtze River, which downstream is about 1,000 to 20,000 meters wide. Related to flow-field areal size is the issue of what size of tracer particle is sufficient for determining flow fields. Yet to be determined is the required or optimum size of tracers for different size flows.

Figure 1.1: Yangtze River downstream of the Three Gorges Dam, China

1.3 Objectives

The LSPIV method has much promise as a fairly fast way to obtain whole-field measurements of water-surface velocities of free-surface flows. CSU's Hydraulics Laboratory wishes to implement this method. Accordingly, the following objectives were set for the present study:

1. Apply the LSPIV technique for use in CSU's Hydraulics Laboratory, especially to two existing flume projects underway in the laboratory; and,
2. Determine how tracer size influences LSPIV accuracy in measuring flow velocity.

These two objectives are important steps in developing the LSPIV method such that it can be routinely applied as a method commonly used in CSU's Hydraulics Laboratory.

1.4 Approach

The study comprised the application of LSPIV to two sets of flume experiments conducted in the laboratory. A key part of the application was the use of the software Fudaa (https://forge.irstea.fr/projects/fudaa-lspiv) for converting video images of LSPIV. This software can be downloaded freely from the website cited. The experiments involved two different flow fields formed in channels formed with erodible alluvial beds:

1. Flow through a series of channel contractions and expansions; and,
2. Flow around and over a bendway weir in two depths of flow.

The flow fields were at different areal magnitudes, and required different settings for video-camera position and size of tracer particle used. The experiments with different sizes of tracer particle were done using the smaller flow field; the flow field was associated with the series of contractions and expansions. Paper pieces, produced by simply cutting up a sheet of paper, were used as the tracers for both experiments. The required water flow was set in each flume using either a pump with speed controller (contraction and expansion) or gravity feed from Horsetooth Reservoir. Once the flow had attained the discharge and depth prescribed for the experiment, the tracer particles were dispersed more-or-less uniformly on the water surface over the approach flow within the flume. Video-camera records were recorded to capture the displacements of the particles on the water surface of the flow by positioning the camera obliquely and vertically to the interest area around the cylinder. LSPIV software was then used on those images of flow and provided free surface velocity by producing two-dimensional vector fields of flow.

1.5 Thesis Structure

The structure of this thesis follows the following sequence of chapters:

- Chapter Two provides a brief summary of experimental approaches to characterize fluid motion, and then discusses the background concepts on unsteady flow and vortex shedding. Various techniques of velocity measurements are also discussed in this chapter. Large-Scale Particle Image Velocimetry (LSPIV) is discussed along with the advantages of this method over other methods of velocity measurement.
- Chapter Three explains the experimental set-up and LSPIV procedure. It also describes the flow fields used in the study, and gives the details regarding the different size of tracers used in the study.
- Chapter Four presents the results of the flow-field measurements and gives the findings of the experiments with different sizes of tracer. This chapter also indicates an optimal size of tracer for use in measuring flow fields by means of LSPIV.
- Chapter Five, Conclusions and Recommendations, gives the study's main conclusions and recommendations.
- The various references cited are listed in the References section of this thesis.

CHAPTER 2, BACKGROUND AND THEORY

2.1 Introduction

This chapter gives a concise summary of the experimental approaches used to measure and characterize fluid motion, and then discusses the likely effects of different tracer sizes on flow field as well as identifies tracer sizes used by researchers in prior studies. Additionally, this chapter compares the LSPIV with other velocity-measurement methods and briefly discusses the advantages and disadvantages of the various methods.

2.2 LSPIV

LSPIV is based on traditional flow-display technology, advanced as a new kind of flow, display-measurement technology using graphic image-processing technology. It combines the advantages of the display-measurement technology (e.g., digitization of images) with rapid data handling so as to give the overall structure and transient image of the surface plane of a flow field.

A sequence of time steps is involved in producing velocity fields by means of LSPIV. The first step involves taking a video record of the flow field of interest. The video record produces a set, or a time series, of flow profile images. Then, an important next step is so-called image orthorectification, which converts the time series of images into set of flow velocity data covering the field of view. Next, follows the core step of the LSPIV technique, image-processing, which is first and foremost a pattern-matching technique, as illustrated in the series of images shown in Figure 2.1. There are two key areas in the image: the interrogation area (IA) and search area (SA). The bigger one is SA, and the smaller one is IA. The two areas have some similarity indexes associated with them. These indices are used to relate similar images in a time

series of video-record frames. Image-processing requires determining the maximum similarity indexes linking two consecutive images, assuming the displacement is tracer move displacement. This action leads to estimating the displacement, dL, of a particular tracer. Knowing the time separation, dt, of video-record frames, this action then quickly leads to calculating the speed of a tracer; i.e., velocity = dL/dt. In the searching process, all IAs in the images are successively applied over the flow area.

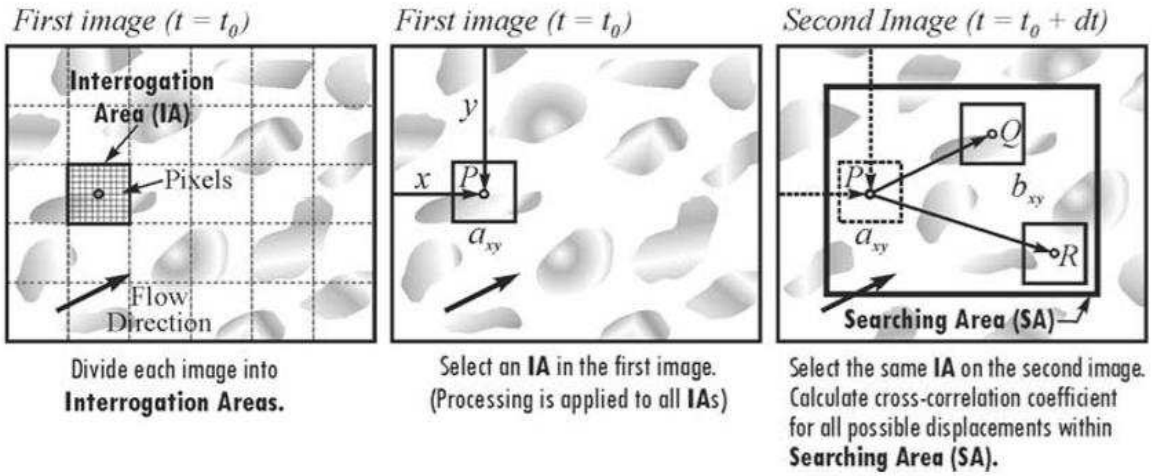

Figure 2.1: LSPIV image processing step

2.3 Experimental approaches

It is useful to briefly summarize the ways used to measure flow velocity. There are two methods often used to characterize fluid motion. They are point-measurement techniques and flow-visualization techniques. These two general methods have their advantages and disadvantages that depend typically on the circumstances of their use. The following section discusses the advantages and disadvantages.

Laser Doppler Velocimetry (LDV), Acoustic Doppler Velocimeter (ADV), hot-wire and hot-film anemometry and pitot-tube (pressure-difference) are used commonly as methods for point-measurement of velocities. However, they only can provide accurate data information at a single point at a time. These methods are well document in many references, including Muste et al. (2017). Many time-consuming measurements are needed to develop a broad overview of a flow field which at present cannot be provided. Flow visualization techniques, however, can help obtain an overview of flow velocities and flow paths in a flow field. These methods include the use of smoke wires and dye tracers. The drawback of these visualization methods is that they are are only for visualization purposes, and typically do not yield quantitative information about a flow field.

A method that combines the ability to quantify and visualize a flow field — i.e., has the attributes of point measurement techniques and flow visualization techniques — is Particle Image Velocimetry (PIV). In recent years, PIV has been advanced for use measuring and visualizing velocities in large-scale flow and field measurements, and has become suitably named Large Scale Particle Image Velocimetry (LSPIV). LSPIV is an effective and promising technique that can be used in field or laboratory conditions to get the overview of a flow fluid. In addition, LSPIV is a promising method for accurate measurement of fluid velocities in various experiment situations, but this potential is still being explored and tested.

2.4 Tracer particle selection

Many conditions, including variations in aerial extent, flow complexity and flow turbulence, occur in field and laboratory experiments. Some laboratory experiments involve only small-scale flows and some involve very turbulent flows, sometimes with air entrainment. Therefore, LSPIV use can be limited to conditions of large-enough flows and flows whose water

surface is not overly turbulent so as to disrupt the movement of tracers or greatly lengthen the travel distance of a tracer. The flows usually must be stable and surface flows have to be related to flow velocities over the body or depth of flow. Some experiments are conducted with natural rivers, which can involve many uncertain factors that can contribute to measurement error, like wind, temperature, the presence of floating obstacles (e.g., logs) or animals (e.g., fish), etc. Therefore, researchers must use distinct size and distinct material for tracers for different experiments in order to get the measurement accuracy needed.

2.4.1 Tracers for curved flows

Most flows involve curvature of flow to some extent. It is useful to relate tracer size to curvature of flow, or in other words, the proportion between diameter of curvature, D, and nominal diameter of tracer, d. Table 2.1 below indicates seven considerations in this regard.

Table 2.1: Values of d/D used for tracer particles in prior studies of flows involving curved paths

Approach mean velocity, U (m/s)	Maximum size of TRACER particle, d (mm)	d/D	Curvature diameter, D (mm)	Re ($\times 10^4$)	Fr ($\times 10^{-3}$)
0.39	12.19	1/50	609.50	23.68	5.04
0.39	12.19	1/38	463.22	17.99	5.79
0.39	9.6	1/32	307.20	11.93	7.10
0.34	12.17	1/50	608.50	20.61	4.40
0.34	6.11	1/75	458.25	15.52	5.07
0.34	4.08	1/75	306.00	10.36	6.21
0.28	11.2	1/41	459.20	12.81	4.17
0.28	6.4	1/48	307.20	85.67	5.10
0.28	2.93	1/75	219.75	61.28	6.03

The first consideration concerns the mean velocity of approach flow to be measured using the LSPIV method. A further consideration is the approximate maximum size of the tracer used; prior experiments in laboratories have used tracers whose max diameter is 12.2mm. Yet another consideration is the proportion between the diameters D and d, defined above. Prior studies indicate ratios in the range of about d/D = 1/75 to 1/30; the prior studies have used D = 0.22m to 0.61m. A fifth consideration is the Reynolds number of flow in a curved path, such as around a cylinder. In this regard the Reynolds number is useful: i.e.,

$$R_e = \frac{DV}{\nu} \tag{2.1}$$

Also, to be considered is the Froude number of flow; i.e.,

$$F_r{}^2 = \frac{V^2}{gD} \text{ and } F_r = \frac{v}{\sqrt{gD}} \tag{2.2}$$

According the data from prior studies, the mean approach velocity does not need to relate directly to the ratio d/D, and it does not have direct connection with maximum size of seed particle or cylinder diameter.

2.4.2 Tracer size for straight flows

According to the papers summarized in Table 2.2 below, various different sizes and kinds of tracers have been used by prior experimental studies. It is useful, for the purpose of this study, to briefly review the sizes of tracers used for prior studies.

Table 2.2: Tracer material and size

#	Tracer material	Tracer size(mm)	Tracer density (kg/m^3)	Flow-field width (m)	Reference
1	Black dye, packing peanuts (starch foam), peanut bubbles (dissolved starch foam), soap bubbles	2.9-12.2	< 1000	3.62	Basnet and Ettema, (2011)
2	White floating cylindrical polypropylenes particles	3.4	960	4.00	Kantoush and et al, (2011)
3	Hollow cylindrical polymer particles	2.4	1007	4.00	Kantoush et al, (2011)
4	White floating oatmeal	50	<1000	5.70	Creëlle et al, (2016)
5	White Styropor expanded polystyrene beads	2	Very light	0.89	Fox and Patrick, (2008)
6	Air-bubbles	5	<1000	0.90	Peltier, Dewals and et al. (2015)

According to the prior-study information summarized in Table 2.2, tracer size is practically always smaller than about 10mm in diameter, and tracer density is usually smaller than the density of water (i.e., buoyant tracers are used). Further, tracers should be easy to obtain, observe and distinguish from various impurities. Also, tracers should not be expensive, as they usually are lost during or after an experiment.

2.5 Sidewall effect on water-surface behavior

Both of the flow experiments (like the bendway wire), conducted with laboratory flumes, had a sidewall effect. This effect essentially is due to reduced velocity of flow close to a wall, and to possible consequences of surface tension, which could cause tracers to adhere to a flume wall; these effects can be called "sidewall drag." Therefore, it was important to ensure that the LSPIV method did not give results influenced by sidewall drag on tracer particles. Figure 2.2

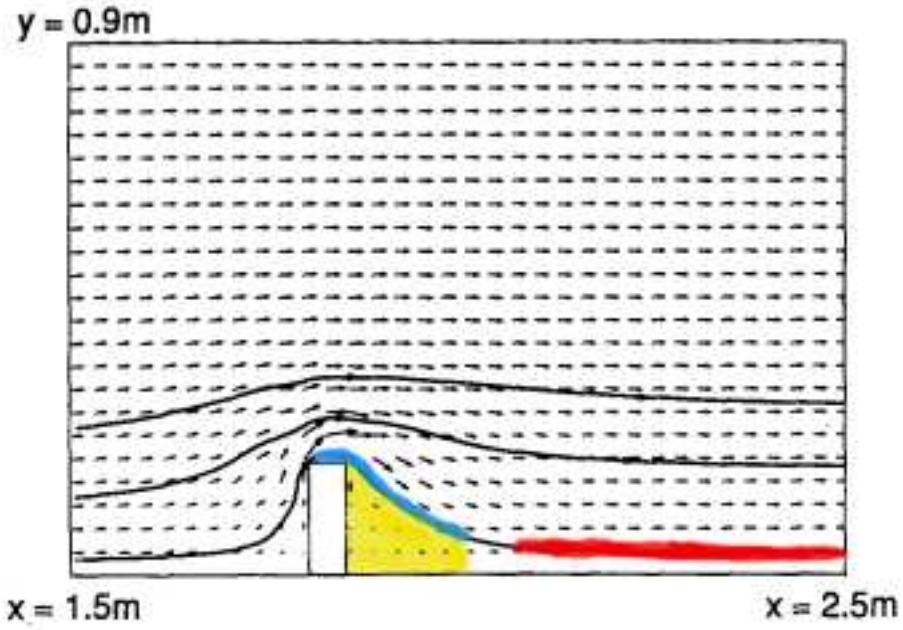

Figure 2.2: sidewall water surface behavior

below shows the influence of side-walls on the simple flow field at a spur extending from a sidewall. The figure also shows some of the flow field complexities that can arise often in laboratory and field flows. In this figure, the blue line indicates flow contraction and separation; the yellow area is a flow- recirculation region; and, the red line indicates a separated shear layer. Tracers can accumulate in the separation region, and they may be in contact with the flume wall in the shear zone, thus giving incorrect values of local velocity magnitude.

2.5.1 Flow around an object that contracts flow

A common flow situation involves flow around an object that contracts flow and thereby gives rise to changes in flow direction (or flow curvature). The usual flow features involve flow acceleration around the contracting object, and then the formation of a flow separation region. Also, flow-separation vortices are generated as flow passes around the contracting object, forming a shear layer in which flow velocity changes at a relatively rapid rate. These flow features should be clearly defined in the flow field defined using LSPIV. Consequently, flow tracers should not blur or make unclear these flow features; i.e., the tracer used should not be so large in size compared to the flow feature that it causes the flow feature to be blurred in the LSPIV image.

Flow separation from the body of an obstacle creates a low pressure area. Then downstream flow draws fluid back into this region from the main flow. As a result, it will create a circulating vortex or pair of vortices. This situation results in a significant increase in resistance as compared to the case where the flow remains connected to the surface, because energy is taken from the flow. LSPIV is potentially useful for delineating areas of flow separation. Boundary layer separation is the separation of the boundary layer from the surface into a wider wake. The boundary layer separation occurs when the boundary layer closest to the wall or leading edge is reversed in the direction of flow. When the shear stress is zero, the separation point is defined as the point between the forward and backward flow. The entire boundary layer is initially suddenly thickened at the separation point and then forced away from the surface by its reverse flow at the bottom.

2.6 Velocity measurement techniques

As the topic of velocity measurement is extensively discussed in numerous existing publications (e.g., Muste et al. 2017), the present summary is kept brief.

2.6.1 Pitot Tube and Acoustic Methods

The Pitot tube is a much used and well-understood instrument that measures velocity in terms of a pressure difference between a local ambient pressure head and the pressure head generated by the approaching flow at a point. The pressure head equals the local pressure head plus the dynamic head associated with water motion. The difference in pressure head thus equals the dynamic head, form which the local velocity is then determined. Similarly, Acoustic Doppler Velocimetry (ADV) through measuring Doppler frequency-shift to determines the velocity and direction of flow. These are just two different ways to determine velocity of water flow at a point within the body of a flow. LSPIV, of course, through measuring the displacement of floating tracers, only gives points velocity at the water surface.

ADV, to explain further, uses acoustic waves emitted into a flow. The waves are scattered by water particles in the flow, and thus makes use of what is called the Doppler Effect; i.e., this (or the Doppler Shift) is the change in frequency or wavelength of an acoustic wave for an observer who is moving relative to the wave source. This ADV operation uses the transmitter and the receiver to record the Doppler Shift that is related to the flow rate. Both the Pitot tube and ADV are intrusive devices and therefore may affect the local flow direction in the case of relatively small-scale flows. Also, the Pitot tube just gives a velocity magnitude and cannot determine the direction of a flow velocity.

2.6.2 Particle Image Velocimetry (PIV)

Particle Image Velocimetry (PIV) can determine instantaneous values of velocity within a body of flow by measuring the displacement of tracer particles immersed within the body of flow. It thereby gives values of velocities in two-dimensional flow fields. Further, the PIV measurements are non-intrusive. The PIV method involves a video camera, an optical arrangement to support the video camera, a high-power laser and the seeding particles. PIV is an especially useful method of flow velocity measurement, because it does not need to place the measurement instrument in the flow, and it is simple, efficient and convenient to use (e.g., Aya et Al., 2002). Besides the advantage of being non-intrusive, PIV has two main advantages over other velocity measurement methods:

1. Measuring the two-dimensional instant velocity distributions and velocity direction; and,
2. Measuring the two-dimensional continuous velocity distributions.

However, PIV has its challenges or limitations. It is relatively difficult to set up, and requires clear water, and tracers that are neutrally buoyant. PIV was developed for use in laboratory situations only, perhaps for a very limited range of field-flow situations where access is facilitated to observe the flow. However, the PIV method cannot be used for large river flow in which flow visibility is limited, or in coastal flows, and is not useful for flows occupying a large area.

2.6.3 Large-Scale Particle Image Velocimetry

LSPIV can non-intrusively be used to get velocity values in a two-dimensional vector field that is either uniform or non-uniform, and steady or unsteady, and over a relatively large area of flow. It is useful for laboratory and field applications. It uses the same method to

measure velocity as does the PIV method, but it can be used in the large scale flows. LSPIV through two successive digital images separated by a known time interval, such as frames in a video-camera. The use of tracers to measure flow-surface velocity is based on the image technology used for PIV (Fox and Patrick, 2008). So LSPIV has the advantages of PIV, but is a more practical method that can be used mostly on the sea or river. Further, its cost is modest and lighting requirements are less stringent than those needed for PIV (e.g., Aya et al., 2002).

Several studies show that the LSPIV method can used successfully and efficiently for large-scale flows in laboratory or field conditions to measure flow velocities. Fujita (1998), for example, illustrates LSPIV use to illuminate the flow fields in several hydraulic engineering applications related to large bodies of water. His illustrations include the distribution of pollution plumes in river and coastal areas. Other examples concern sediment movement in parts of watersheds, environmental degradation erosion, flooding, and ice-mitigation schemes. In these different examples, LSPIV measurements revealed mean flow features, regions of eddy or reversed flow, and were useful for mapping flow distributions within turbulence scales. Estimation of these quantities by other velocity-measurement methods faced some problems involving inherent difficulties and considerable experimental errors. Also, the potential use of other methods would incur much expense.

There are four basic steps involved in conventional LSPIV: flow visualization, illumination, image recording and image-processing. As LSPIV recording always involves a large area, an additional step is image ortho-rectification, which aims to reduce the influence of oblique angle viewing of the flow surface. Additionally, LSPIV usually involves delineating the flow field of interest, selecting the right tracer particle, and then determining how to place the tracers on the flow surface on the flow. It also entails recording a digital video by means of

video camera so as to get images by the necessary process to calculate the flow velocity by the successive images. Estimation of flow velocities also involves selecting an averaged time with which to calculate the free surface velocity then determine the characteristics of the flow.

The co-relation of flow patterns within an interrogation area (IA) fixed in the first image is calculated for the same-sized window within a larger search area (SA) selected in the second image. The window pair with the maximum value of the correlation taken to give the most probable displacement of tracers between two consecutive images. After finding the distance between the centers of the respective small window, and dividing it with the time difference between consecutive images (e.g., 33.33 milliseconds for the experiments in the present study) velocity can determined. This searching process is applied successively to all IAs in the image (Muste, 2008). The last calculation is to determine the velocity of flow at a location. This calculation is applied to each measurement location in all the IA images.

CHAPTER 3, APPLYING THE LSPIV METHOD

3.1 Introduction

This chapter first describes the experiments, and their laboratory arrangements, used for implementing and checking the accuracy of the LSPIV method at the CSU Hydraulics Laboratory. Two distinctly different-sized channels or flumes were used for investigating the application of the LSPIV method and to calculate flow-surface velocities using the LSPIV measurement. The first experiment focused on the how tracer size affects the accuracy of velocity measurement by means of the LSPIV measurement; different size tracers were used to measure the flow velocities in a relatively small-size channel. The second experiment applied the LSPIV method to determine the water-surface flow field associated with flows around and over a bendway weir at which local scour developed in the erodible sand bed upon which the bendway weir was placed. This latter experiment involved a much larger flume, and thus flow field, and so tracer size was much less of an issue.

Further, this chapter discusses how to obtain useful tracers for LSPIV use. Useful tracer size is defined in terms of tracer area, perimeter and length relative to the dimensions of a flow field. This study uses a nominal diameter or side-length of tracer to indicate tracer size. The outcome is useful guidance for LSPIV use on how to choose an affective tracer for use in various flow situations.

This chapter also discusses the general sequence of steps needed to apply the LSPIV method for measuring water-surface flow velocities. It contains preparing taking setting running the software to calculate the velocity. On these steps, there are some tips to be summarized which need to be considered when using the LSPIV measurement in the future.

3.2 Dimensional analysis

In order to apply the LSPIV method for the two experiments it was necessary to use suitably sized tracer particles. This section uses dimensional analysis to identify useful non-dimensional parameters for this purpose.

There are a total of eight dimensional variables that can be identified for this purpose. The essential variables are shown in Figure 3.1, and include the following variables (dimensions are indicated in brackets):

V: the velocity of water at the water surface (LT^{-1})

g: acceleration of gravity (L^2T^{-1})

d: the diameter of the particle (L)

ρ_p: the density of the tracer particle (ML^{-3})

D: the diameter of the obstacle (L)

ρ_f: the density of water (ML^{-3})

ν: the kinematic viscosity of water (L^2T^{-1})

σ: the surface tension of water (MT^{-2})

y: the width of the channel or flow field (L)

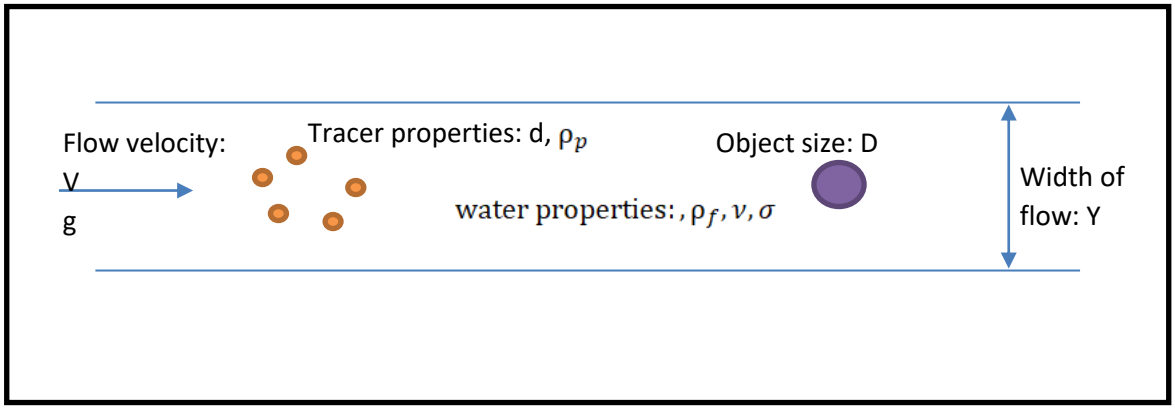

Figure 3.1: Variables involved in a typical water-surface flow field

For finding the relationship between particle material and experimental accuracy, it is useful to define the diameter of the tracer particle, d, as the main dependent variable. The functional relationship f_1, then follows:

$$d = f_1(V, g, \rho_p, D, \rho_f, \nu, \sigma, Y) \tag{3.1}$$

This equation expresses the variables that need to be considered when selecting the correct or necessary size of tracer particle in order to accurately measure flow field velocities. Note that the properties of water vary with water temperature, and that a constant water temperature is assumed. As there are three independent dimensions – mass ([M], length [L], and time [T]) – and eight independent variables, there should be five non-dimensional, independent 5 parameters. The analysis selects the following three repeating variables:

$$D = [L]; V = \left[\frac{L}{T}\right]; \ \rho_f = \left[\frac{M}{L^3}\right] \tag{3.2}$$

Then, standard dimensional analysis gives five non-dimensional parameters for sizing tracers used in LSPIV;

$$\frac{d}{D} = f_2\left(\frac{gD}{V^2}, \frac{\rho_p}{\rho_f}, \frac{\nu}{DV}, \frac{\sigma}{\rho_f V^2 D}, \frac{Y}{D}\right) \tag{3.3}$$

Simplification and analysis, further gives

$$\frac{d}{D} = f_3\left(\frac{V^2}{gD}, \frac{\rho_p}{\rho_f}, \frac{DV}{\nu}, \frac{\rho_f V^2 D}{\sigma}, \frac{Y}{D}\right) \tag{3.4}$$

With the well-known identities, (F_r is Froude Number, R_e is Reynolds Number and W_e is Weber Number)

$$F_r{}^2 = \frac{V^2}{gD}; \; R_e = \frac{DV}{\nu}; \; W_e = \frac{\rho_f V^2 D}{\sigma} \tag{3.5}$$

So, equation 3.5 becomes

$$\frac{d}{D} = f_4\left(F_r, \frac{\rho_p}{\rho_f}, R_e, W_e, \frac{Y}{D}\right) \tag{3.6}$$

The dimensional analysis given above indicates that d/D is an important consideration that will influence the accuracy of velocity measurement by means of the LSPIV measurement method. Also, the analysis indicates that the selection of d/D is affected by the parameter W_e, which is an important term introducing the influence of surface tension.

3.3 Experiments

As mentioned above, two different channels or flumes were used in this study. The first flume was a 4.0ft-wide and 2.5ft-deep flume channel. It was used to test the relationship between measurement accuracy and seed particle size. The second flume was the so-called Tarbella flume (named by CSU's Hydraulics Laboratory), which is 20.0ft wide and 8.0ft deep. It was used, with the LSPIV measurement method, to determine the flow field over and around a submerged bendway weir, a structure formed of rock and used to control the alignment of alluvial channels. This section describes the flumes and then describes the procedures used for each experiment.

3.3.1 The four-foot flume channel

Figure 3.2 shows a photograph of the 4.0ft-wide flume channel, which is 60.0 feet long and 2.50 feet deep. In metric dimensions, this flume may be stated as being 1.22m wide, 18.29 m long and 0.76 m high. The flume was set up for an experiment conducted for another study concerning sediment movement in a series of contractions and expansions. The flume width varied in waves or wavelengths of 1.7m. The smallest width of the flume was 0.443 m and largest width channel was 1.139m.

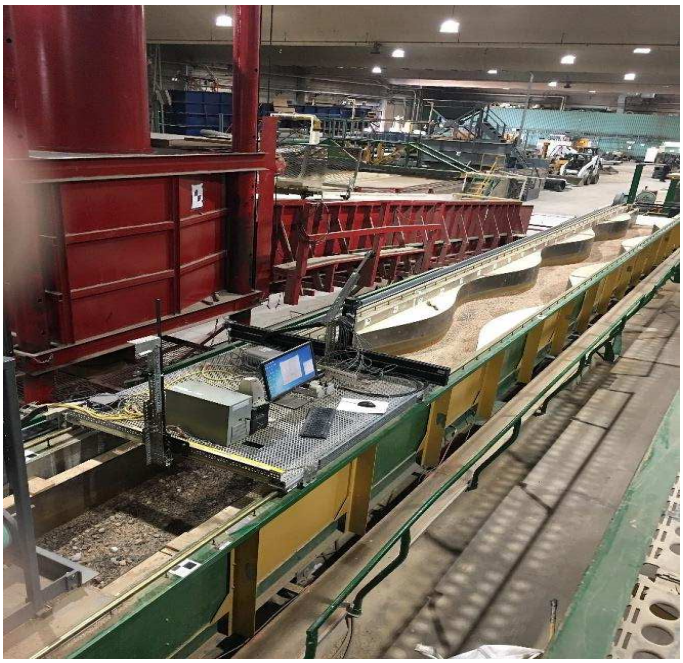

Figure 3.2: A view of the four-foot flume channel (in the foreground)

The extent of scour or sediment accumulation along the flume's bed can influence the flow field along a contraction and expansion sequence. Accordingly, this variation in bed topography along with the contraction-expansion geometry of the flow influences that flow field along the flume. Of interest was the ability of the tracers (of differing size) to reveal the water-surface flow field along the sequence, which produced zones of flow acceleration and

deceleration, but had no zones of flow separation that could entrap the tracers. The flume's maximum slope is 0.50, but slope was set at 0.0075m/m for the present experiment.

There are two discharge lines which can supply water to the 4-foot flume. The 6-inch bypass line can supply discharges ranging from about 0.25 to 5.0 cfs (0.007 to 0.142 m^3/s), and the 24-inch Annubar line can supply discharges ranging from about 4.0 to 25 cfs (0.113 to 0.708 m^3/s). For this study, the discharge was set at 2.55 cfs (0.072 m^3/s), and so was supplied by the bypass line shown in Figure 3.3. Because this channel is small, and the flow field is correspondingly small in surface area, the tracer particles were selected to be relatively small, too. If the discharge was to be very large in this flume, the flow will become rather turbulent and wavy, making the LSPIV method of uncertain usefulness.

Figure 3.3: The 6-inch bypass line controlling flow along the flume

The dimensions of the flow field of interest for this study were 9.19 ft long (2.76 m) and 3.94 ft (1.20 m) wide. A sequence in the middle of the flume was chosen for the measurements. Because the water discharged into the flume by the flume's pump was a little turbulent, the water profile at the start area of the flume was not steady enough for this study. Also, at flume's

outflow, the flow was affected by the outflow-control gate and was not of interest. For the study area, the water-surface profile was only influenced by the flumes sequence geometry and the bottom elevation variation of the bed. Additionally, the bottom roughness variation, shown in Figure 3.4, affected the flow distribution. Consequently, the water profile varied along and across the test section of the flume.

Figure 3.4: A view of the bottom of the research area (LSPIV interrogation area) in the channel

To capture the total research area, or interest area of flow, on the video record, it was necessary to position the camera at a suitably high location. Such positioning also reduced the orthorectification requirement; having the camera close close to the channel would have meant greater need for orthorectification. Figure 3.5 shows the location used for getting the video record. The tracers were dispersed on to the flow at the start of the channel when the video record was being made.

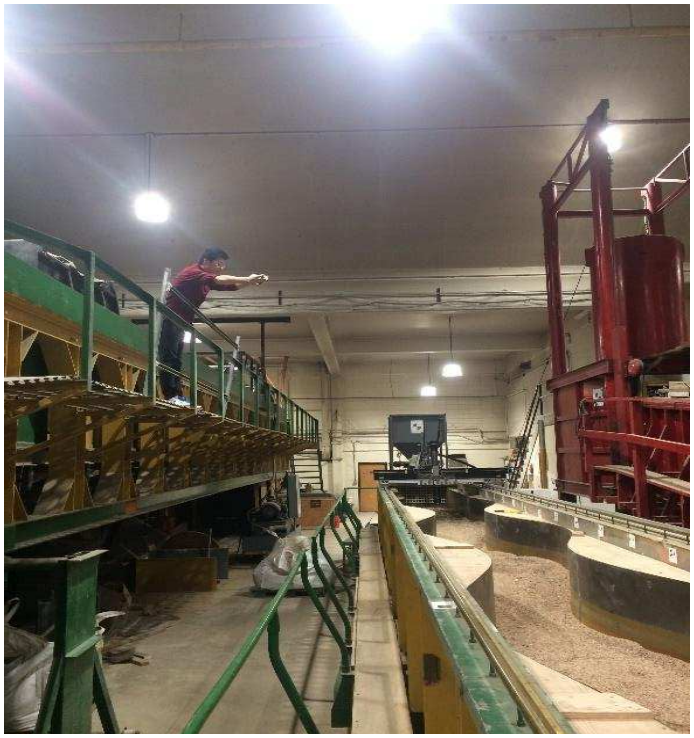

Figure 3.5: Place from which to take the video record of the tracer drift on the flow field

3.3.2 The Tarbella flume channel

The Tarbella flume is a comparatively large channel, and is 20.0 ft (6.10 m) wide, 180 ft (54.86 m) long and 8.0 ft (2.44 m) high. The bottom of the channel has a relatively smooth, concrete finish that is of uniform roughness. The bendway weir was placed on the east side of the flume's sediment recess, about 52 ft (15.90 m) downstream from the flume's entrance manifold.

Figure 3.6 shows the dimensions of the bendway weir. The bendway weir was built from 6-in-diameter rock. Figure 3.7 is a photograph of the Layout of the bendway weir in 20ft-wide flume. Also shown is the bendway weir placed on a sediment recess in the flume's invert.

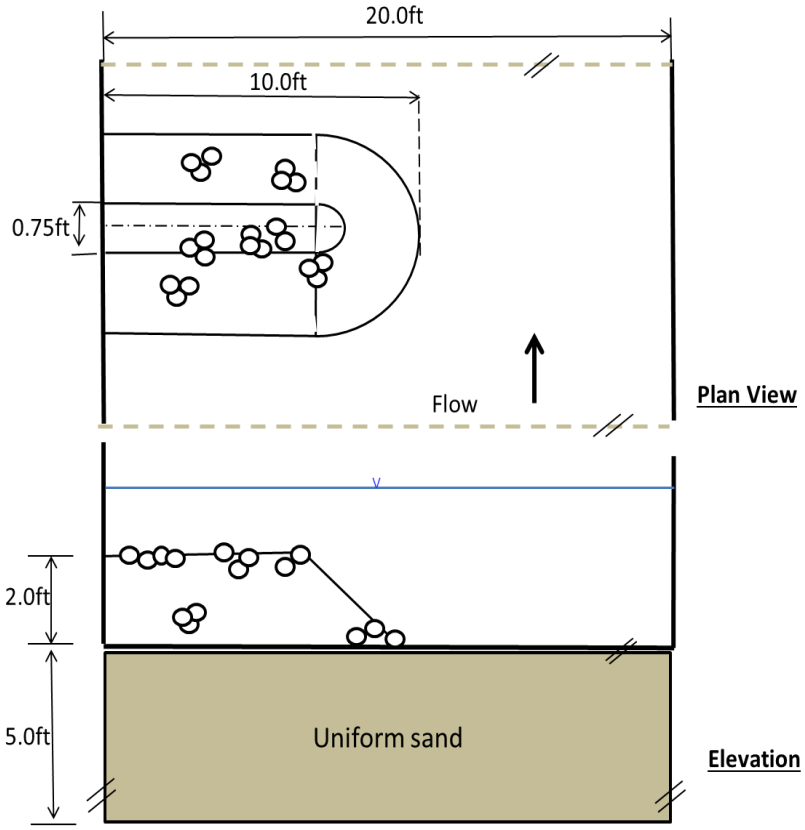

Figure 3.6: Details of bendway weir dimensions

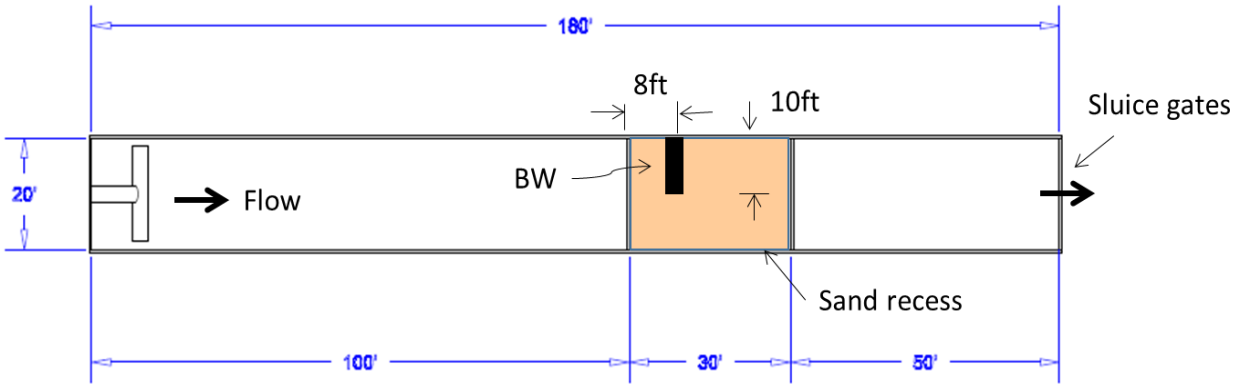

Figure 3.7: Layout of bendway weir in 20ft-wide flume

The discharge used for the test in the Tarbella flume channel was 87.0 cfs (2.35 m^3/s). The flume's maximum discharge was about 200 cfs (5.46 m^3/s). The research area on this project is extended along a 29-ft length of flume and encompassed the sediment recess. The test section was about in the middle of the flume, where flow had a steady profile without influence by inflow and outflow conditions. This location enhanced the accuracy by LSPIV measurements, as with a 4-foot steep flume channel. The location for the video filming was selected so that measurements would not be influenced by light reflections from the water surface; the video filming was done in the afternoon. Therefore, it was decided to do the video filming from the flume's instrument carriage on the south side on the channel shown in Figures 3.8 and 3.9. The tracers also were dispersed across the channel by scattering by hand from both sides of the channel. The tracer coverage across the channel was observed to be sufficiently uniform to enable the LSPIV method to work well.

Figure 3.8: The position used for video-recording from the instrument carriage of the Tarbela Flume

3.4 Tracer-particle size

Four different sizes of tracer particle were used for the first set of experiments involving the 4.0-ft-wide flume. They had length dimensions of 0.275in, 0.40in, 1.20in, 2.0in and 4.0in (0.7cm, 1cm, 3cm, 5cm and 10cm), and are shown in Figure 3.10. Table 3.1 summarizes the dimensions and details. The tracers were made from paper punchings (smallest tracer) and paper tracers carefully cut from sheets of paper. All tracers were made from regular printing paper, which can float on the water, is environmentally friendly (disintegrates), and is easy to observe by video camera. But this paper had one problem, insofar that light reflected from it to influence the result accuracy. On the second set of experiments, use was made of only the largest tracer, because the channel was very wide and the flow swifter than in the smaller flume. Also, use could not be made of the small size seed particle, as it would not be so visible by means of the

video camera. Therefore, the experiments used only the 10cm square tracers for the LSPIV measurements. Each experiment required about 1,000 tracers to create adequate concentration of tracers on the flow and thus lead to accurate velocity measurements.

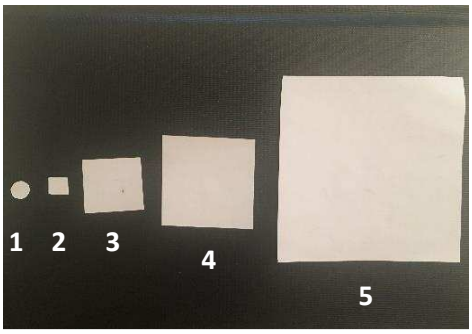

Figure 3.9: The five different sizes of tracer particles used for the experiment with the 4.0 ft-wide flume

Table 3.1: Tracer particle size

	Length of side or diameter (cm)	Perimeter (cm)	Area (cm^2)
1	0.7	2.2	0.39
2	1	4	1.0
3	3	12	9.0
4	5	20	25.0
5	10	40	100.0

3.5 Benchmark setup

The experiments required the use of benchmarks, which are important to establish distances in the photograph images. The video camera did not use a vertical degree perspective. Each data point had to be superimposed on a flat photo which corresponded to image orthorectification. The benchmarks gave data relating to identifiable Ground Reference Points (GRP) that related to positions in the reference image and the real image. The benchmarks were selected with care. First, it was necessary to make sure every benchmark appeared in the viewed

research area. Second, every benchmark had to be easy to be distinguished and located. Third, the distances between every benchmark had to be accurately measured in the real image and reference image.

3.5.1 Four-foot flume

There were eleven benchmarks shown in Figure 3.10. They were used to help with image orthorectification. Table 3.2 gives the data about the positions of the benchmarks.

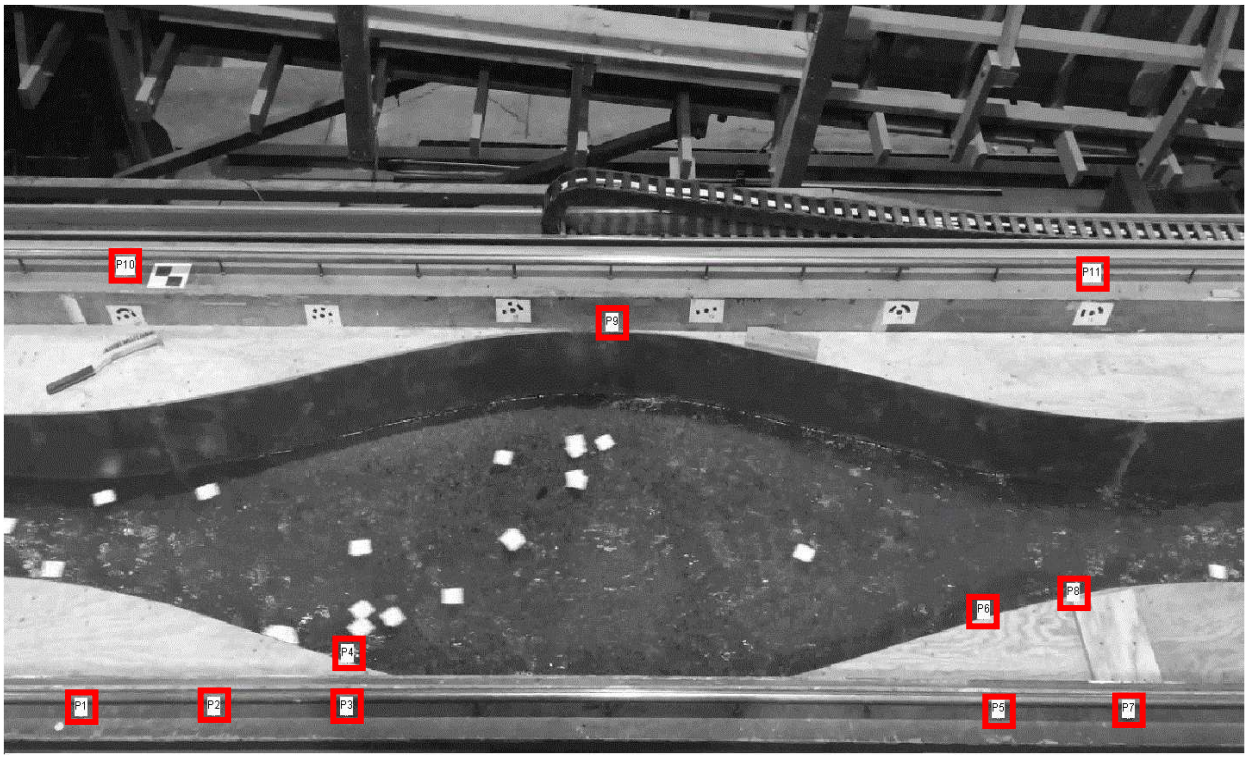

Figure 3.10: Eleven benchmark points (red squares) (5cm square test)

Table 3.2: Benchmarks points data (Four-foot flume)

Index	I	J	Real X	Real Y	Real Z
1	237	112	5.68	0.0	0.0
2	649	114	6.0	0.0	0.0
3	1059	114	6.3	0.0	0.0
4	1062	266	6.3	0.15	0.0
5	3080	105	8.13	0.0	0.0
6	3034	390	8.13	0.22	0.0
7	3482	105	8.48	0.0	0.0
8	3312	443	8.48	0.28	0.0
9	1882	1221	7.21	1.14	0.0
10	377	1385	5.68	1.2	0.0
11	3370	1362	8.48	1.2	0.0

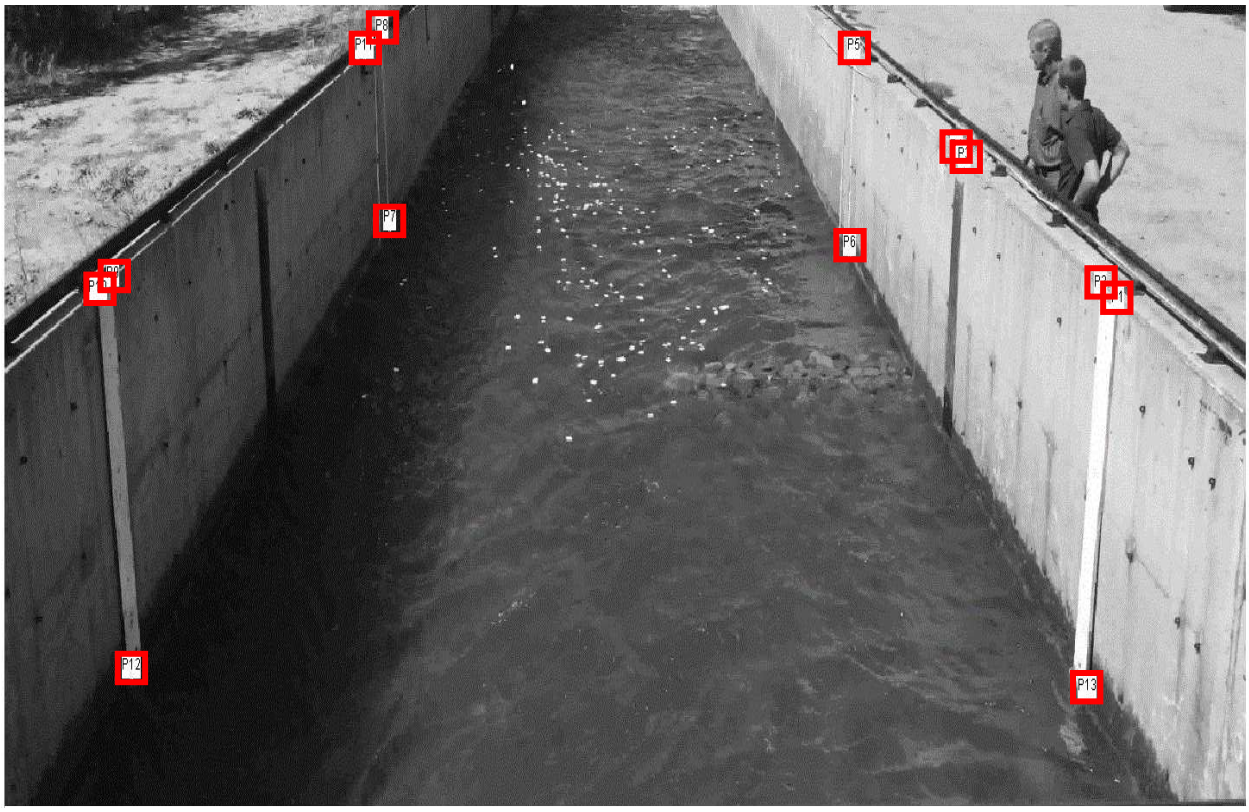

Figure 3.11: The thirteen benchmark points used for the Tarbela Flume experiments

3.5.2 Tarbella flume channel

There were 13 benchmarks shown on Figure 3.11. They helped to define length dimensions in the images and thus enable accurate orthorectification. Data on the positions of the benchmarks are given in the Table 3.3.

Table 3.3: Benchmarks points data (Tarbel Flume)

Index	I	J	Real X	Real Y	Real Z
1	3444	1036	0.0	20.1168	2.4384
2	3391	1069	0.0	19.9339	2.4384
3	2968	1337	0.0	16.7945	2.4384
4	2946	1352	0.0	16.6116	2.4384
5	2627	1563	0.0	12.253	2.4384
6	2613	1152	0.0	12.253	0.8077
7	1190	1206	6.096	11.5824	0.8077
8	1166	1602	6.096	11.5824	2.4384
9	334	1087	6.096	19.9644	2.4384
10	289	1058	6.096	20.1473	2.4384
11	1115	1563	6.096	12.9845	2.4384
12	394	270	6.096	20.1473	0.8077
13	3350	227	0.0	20.1168	0.8077

3.6 Video recording

A key part of the use of LSPIV is recording a suitably detailed video image if the flow field and tracers. Even a simple video camera can do this task. Therefore, the present experiment used a common iPhone 6s model A 1687 to do the video-image recording. The camera had a 4K, 30fps format, such that the image can have a maximum size of 3840×2160 pixels and record 30 images in 1 second. When taking the video, it was important to get every benchmark in the images. Also, it was important not to have other factors to influence the result; e.g., wind, light reflection, and significant waviness of water surface. Also, the camera hand had to be held steady when taking the video so as not to make the video image shake. The use of a smart phone means

that LSPIV measurements can be readily made with commonly available video cameras. The better the camera, then of course greater detail can be interrogated from the resulting video. Also, placing the video on a stand, so that it is fixed in position, helps set video quality.

3.7 Image processing and transformation

After taking the video record, the video-record was then downloaded to a computer. Then software titled VirtualDub was used to extract the images by 30 fames every second from the video. This step required setting up the video-frame rate to be exactly 30 frames/second.

The next step involved choosing suitably continuous images which will be used to calculate velocity by means of the LSPIV measurement. For this purpose, the present study used Xnview software to transform the image format from jpg or gnp formats to the pgm format. This format has 256 gray levels, and is the main format used in the LSPIV measurement software. The 256 gray levels can help reducing errors in estimates because they give great clarity of image and thus better definition of tracers.

3.8 LSPIV software

The LSPIV measurements convert the movements of the drifting free-surface tracers to measurements of the free-surface velocity of flow in the flow field. The LSPIV measurement software used for this purpose (Fudaa) involved the following steps to calculate flow velocities:

1. Begin the software set-up and select the video-record images;

2. Orthorectify the images and define a GRP;

3. Define an interrogation area (IA) and a search area (SA);

4. Form the estimation grid; and,

5. Calculate values of the local velocity at position and determine average values of velocity at positions.

The following sections elaborate these steps.

3.8.1 Beginning and selecting images

The software sets each new test as its own new "project" for analysis. Then for every project, the main values of variables associated with the project should be recorded and saved in the software's documentation. The next step involved choosing a sequence of images that are free of vibration. The images should number about 100, so as to insure the results are suitably integrated. Every image should have the same orthogonal coordinates and use the same benchmarks; doing so helps coordinate the results more accurately. Also, all images need to have the same time interval separation. Further, every image should have visible tracers that are easy to see, and not have other influences, such as intermittent light reflections.

3.8.2 Orthorectification and GRP

In this step, every point in the images is related in position to the positions of the benchmarks. Every point should be the same in the sequence of images and should consistently relate to the benchmarks. This step is important for the orthorectification process. It is possible to change the data on points in the images so as to make sure that the process is correctly implemented and proceeds accurately. To get a good orthorectification takes 10 minimum benchmarks. These benchmarks need to be well distributed in the image, not aligned from the same point, and include rating variable z data if possible. Always set up the bottom of the channel at the zone point of the z coordinate. Then it is possible to define the transformation parameter, and use the software to calculate default values and input the water level after setting

up the benchmarks. The next step is to transform all images using the input data and to calculate the data on positions. Lastly, check GRP in the images that finish the orthorectification. The images can be stretched or shrunk and may be blurry after the orthorectification process, as evident in Figures 3.12 and 3.13.

Figure 3.12: Before the orthorectification process (5cm square test)

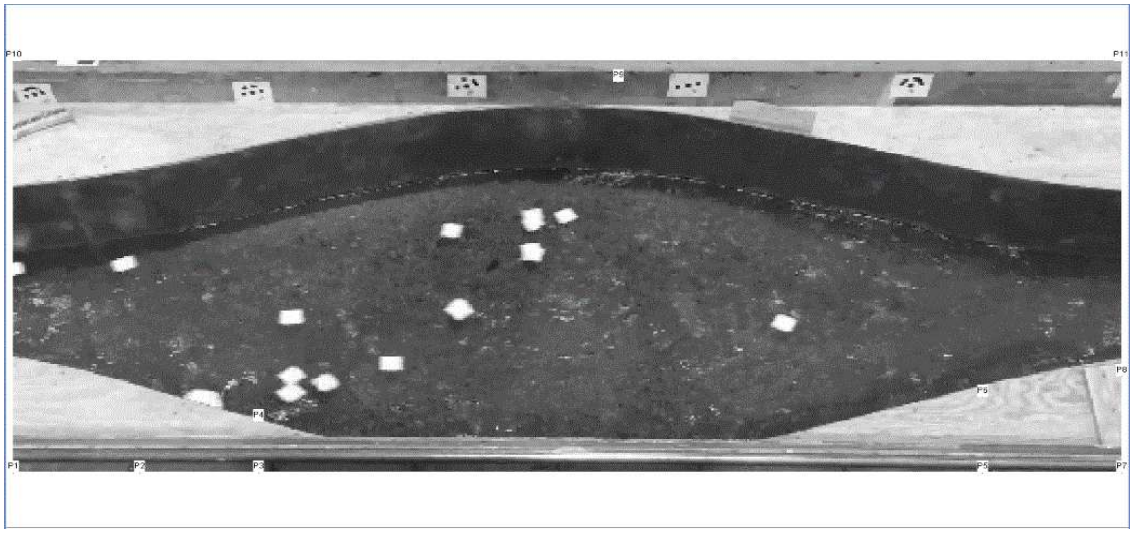

Figure 3.13: After the orthorectification process (5cm square test)

On the first test, the discharges were 2.55 cfs (0.072 m^3/s). Because the discharges were the same when use different size seed particle, every test has the same water level of about 0.8 m.

3.8.3 Interrogation area (IA) and search area (SA) definition

The interrogation area (IA) is a square area that incorporates all the tracer particles and can be representative of the scales of interest within the flow field. It cannot be so big that IA size adversely affects calculation efficiency, but also it cannot be so small that it makes the results not sufficiently accurate enough. Making the IA process more efficient typically involves moving its center position to the center of the region that needs to be interrogated. On the 5-cm square test area, input area size is 0.302 m (54 pix), as shown in Figure 3.14. The center position was moved from J to 240, I to 84. The time step was set at 0.033 s.

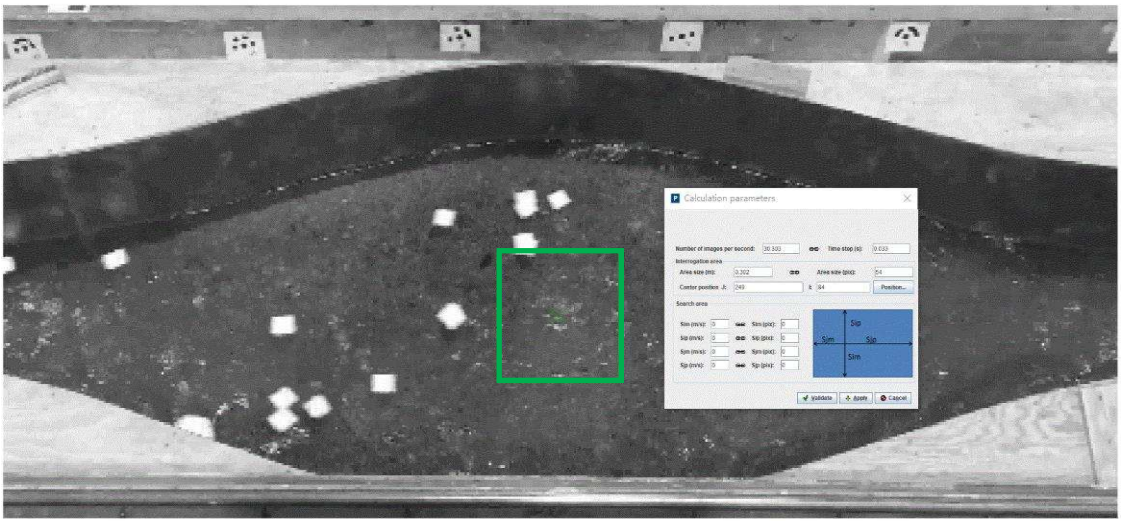

Figure 3.14: Interrogation area (IA) set up and the green area is the interrogation area. (5-cm square test)

The search area (SA) is a rectangle with the same center as the interrogation area. It is an area that shows the center patterns on these continuous images. If the flow has a preferred

direction, the SA can be extended in this direction to make the results more accurate. And the SA is defined by four direction parameters, Sim, Sip, Sjm, and Sjp: i.e.,

Sim: distance from the top of the search area to the center.

Sip: distance from the bottom of the search area to the center.

Sjm: distance from the upstream side of the search area to the center.

Sjp: distance from the downstream side of the search area to the center.

After inputting the SA parameters, a blue area is draws in the image. Figure 3.15 displays the SA parameters set up and SA area.

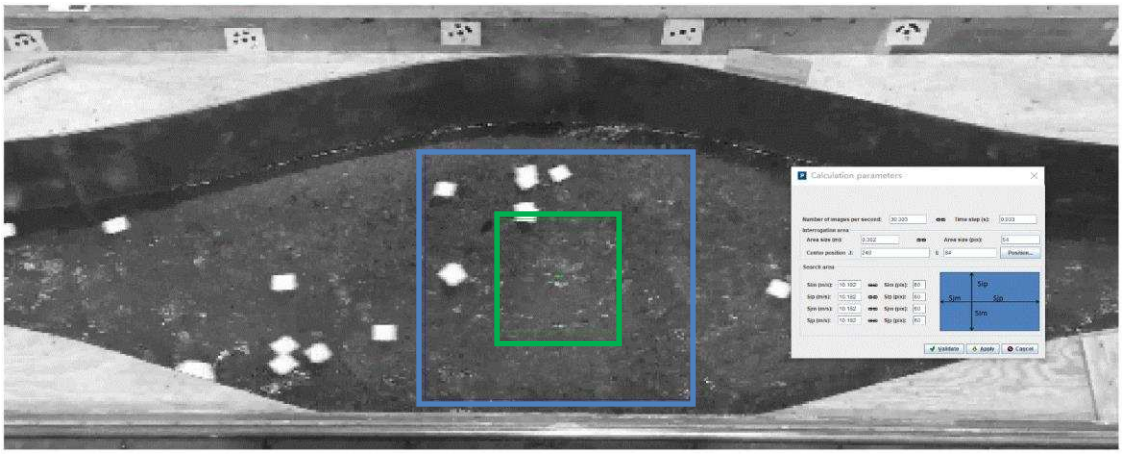

Figure 3.15: Search area (SA) set up and the blue area is the interrogation area. (5-cm square test area)

On the 5-cm square test, the Sim, Sip, Sjm and Sjp comprise 60 pixels. Figure 3.15 displays the SA parameter set-up and SA area. On the SA set-up, there is the need to ensure that all tracers move through this area. Because it measures free-surface flow velocity, only the macroscopic picture is needed. But if a test needs to measure a local velocity or some detailed profiles, the SA must calculate all four parameters to ensure result accuracy.

3.8.4 Defining the grid

A grid set-up is used to define the position points needed for an LSPIV measurement so as to calculate velocity values. It can change the area so as to be comparatively big or small, based on the research area and the test target of interest. The number of points also can be decided based on the test objective. On the 5-cm square test, for instance, the red line is first used to select the whole image. Then, input the number of points in segments 1-2/3-4 is 60, and the number of points in segments 2-3/4-1 is 20, as evident in Figure 3.16.

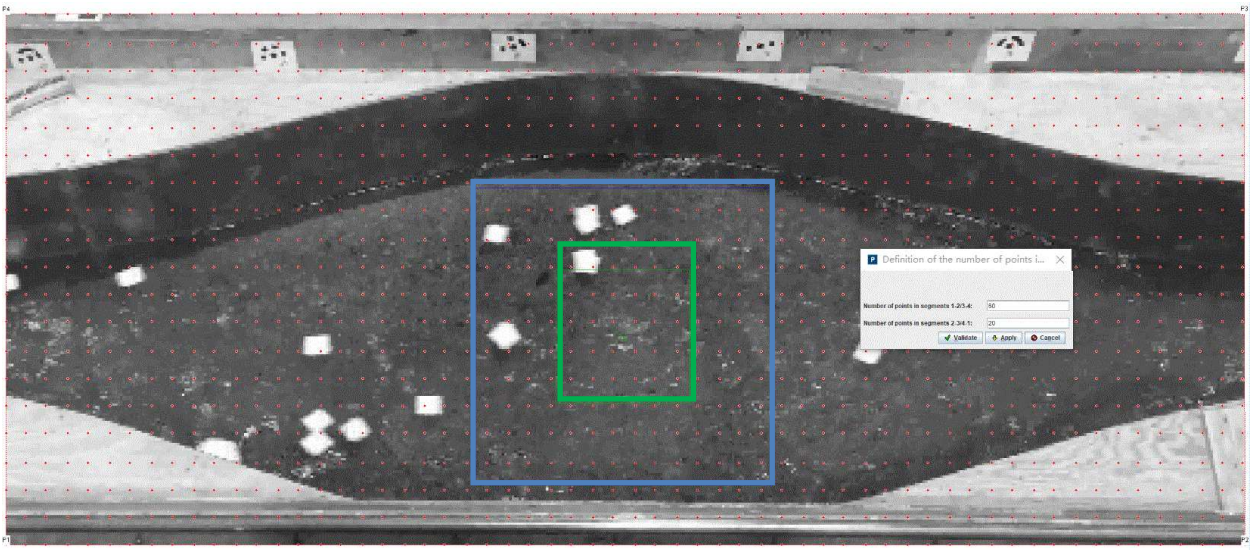

Figure 3.16: Defining the grid and the red points are measurement points. (5-cm square test)

3.8.5 Calculate values of local velocity

After setting up the images and grids suitably, the software can be used to calculate the values of local velocity, which then can be averaged with respect to time in order to give a temporal mean velocity. The image will have several yellow vectors, as shown in Figure 3.17. At the right top of the image, there is a velocity scale plate (software information box), for the

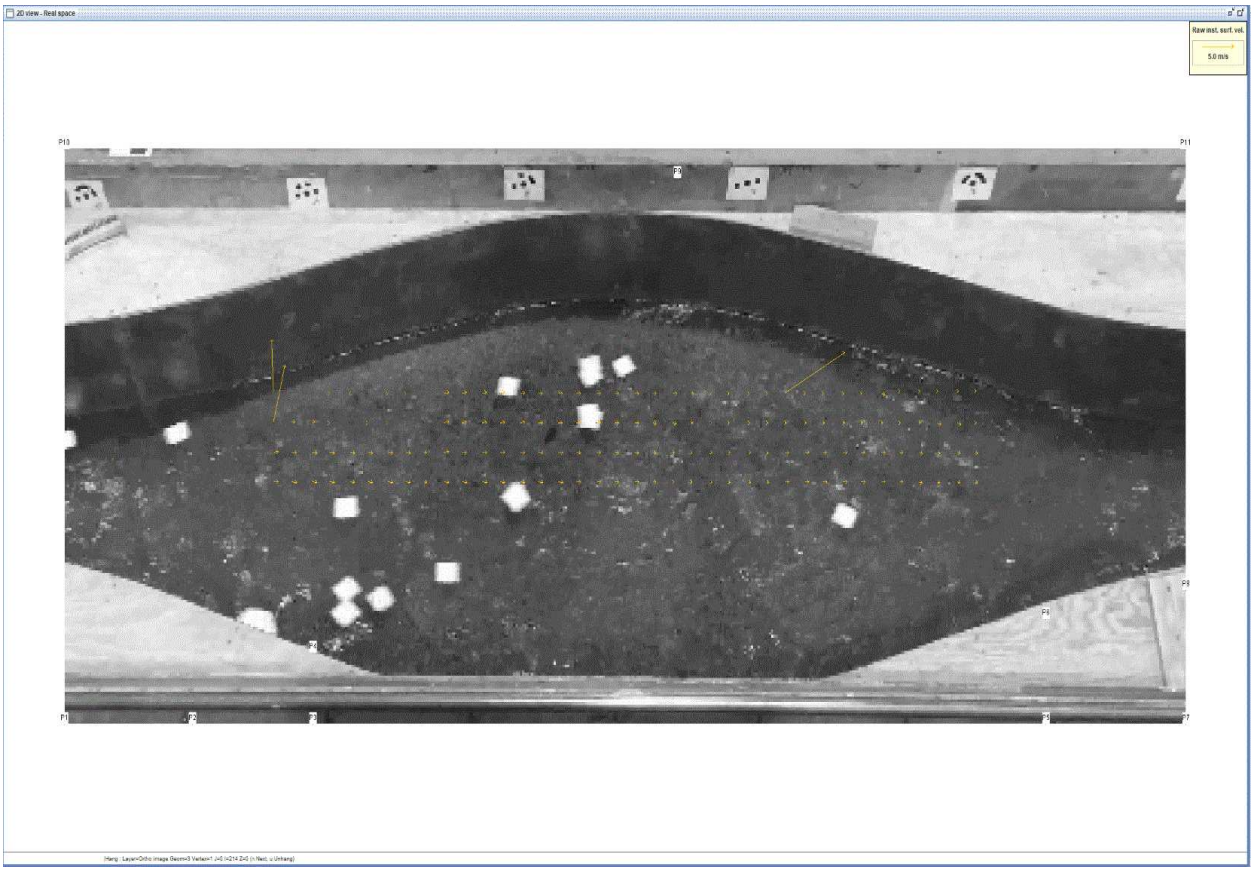

Figure 3.17: Local velocity calculate and shown (5-cm square test)

velocity scale whose length is equal to 5.0 m/s. The information box can be used to determine some vectors that are so big that they are not real, likely because of various factors in the LSPIV method. Therefore, it is necessary to set up the velocity range in order to delete some unreal data (velocity magnitudes or directions) to improve the accuracy of the results. In the 5-cm square test set-up, the velocity magnitude range is from 0.001 to 3.0 m/s; the V_x component magnitude

range is from 0.001 to 3.0 m/s; and, the V_y component magnitude range is from -3.0 to 3.0 m/s. Figure 3.18 displays the average values of velocity obtained from the 5-cm square tests. The red vector shows point velocities in water surface of the flow. On the right-hand top of the image, there is a velocity scale plate. At this image the velocity scale plate is 0.44 m/s.

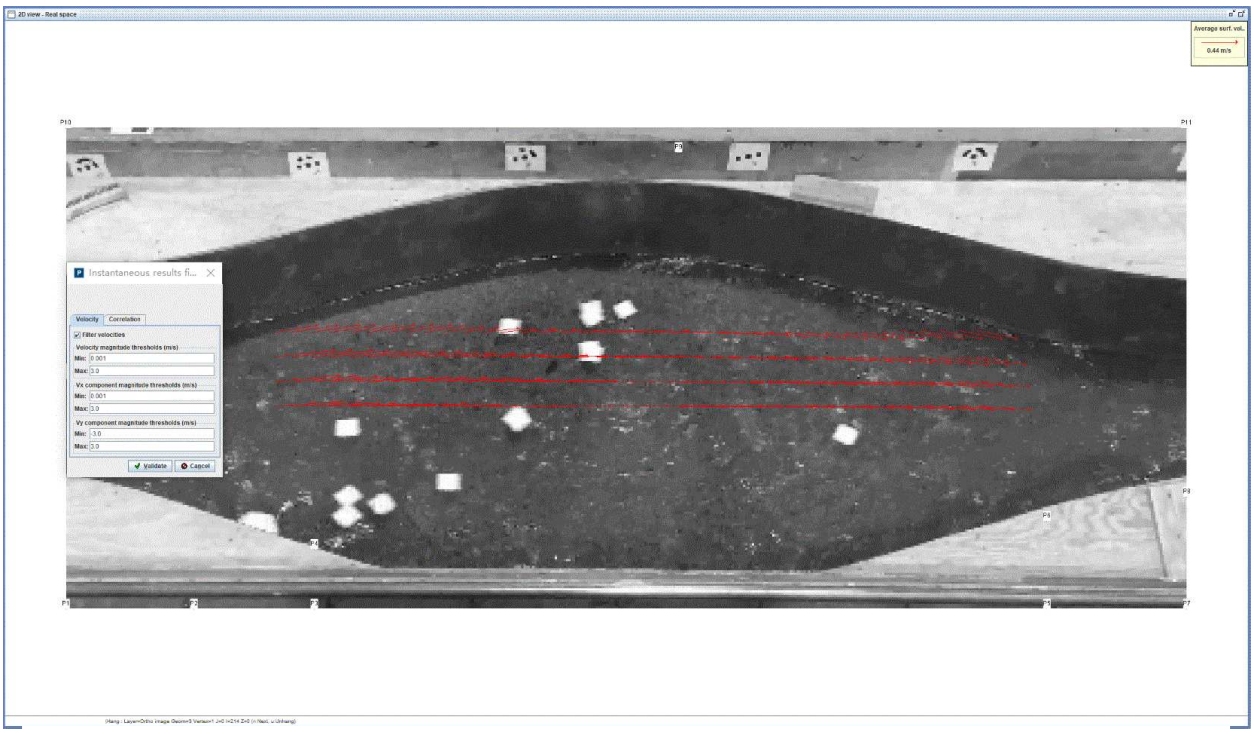

Figure 3.18: Average velocity calculated and shown (5-cm square test)

3.9 Pass line and velocity contour

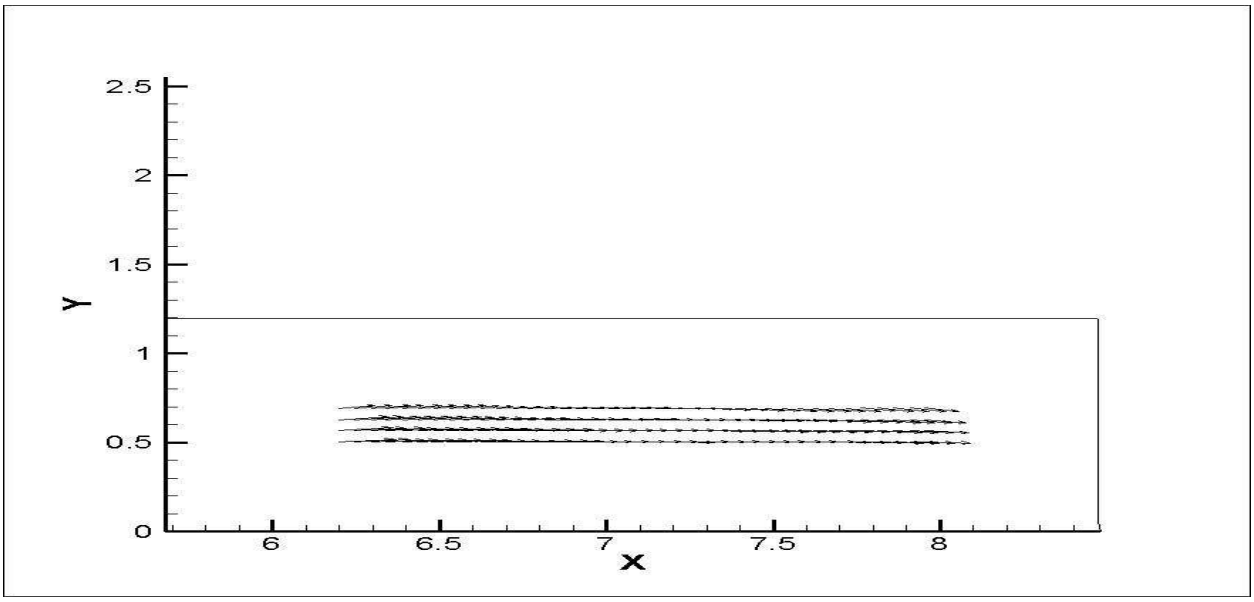

Figure 3.19: Average velocity shown in Tecplot 360 (5-cm square test)

After getting all the velocity data obtained from the LSPIV video images, it is possible to determine and document values of "average_vel.out" in the LSPIV project (for the measurement set). This step requires creating another ".dat" document. It entails defining the input data "X" and "Y" coordinates for the data; the "U" component of velocity on the X direction, and the "V" component of velocity on the Y direction. This step also requires setting up the flow field format in terms of "I=60, J=20, F=POINT". Accordingly, the flow field is displayed using these 1200 points. In the X direction, there are 60 points; and, in the Y direction there are 20 points. Next, this document is imported to the software Tecplot 360, and the command "use these setting for all data sets" is selected. Then, as Figure 3.19 shows, Tecplot 360 can present the velocity vector images, after checking for vectors that are in error and out of range.

By checking the "contour" command, velocity contours will show on the image. The contours are evident as changes in color, as shown in Figure 3.20. Finally, check the

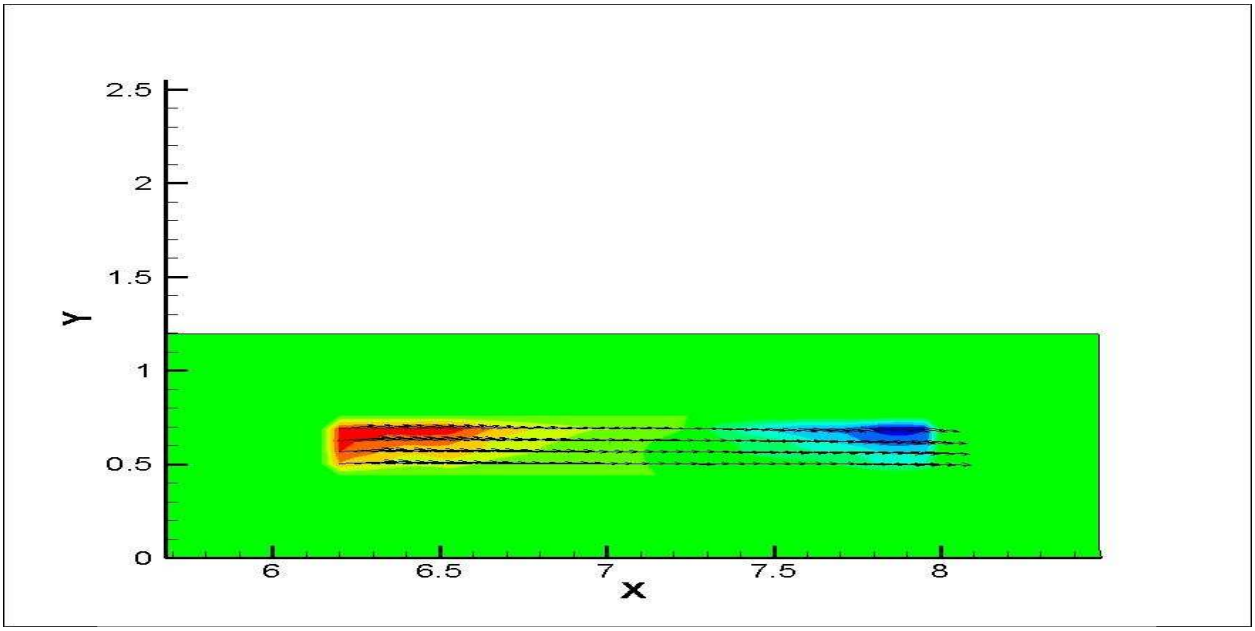

Figure 3.20: Velocity contour shown in Tecplot 360 (5-cm square test)

"streamtraces" command, and choose the points forming the start and end positions. The software will draw the path-lines that run through the line that was drawn before. Repetition of the last proces produces more path-lines until enough are shown that clearly illuminate the flow field. The eventual path-line image is illustrated in Figure 3.21.

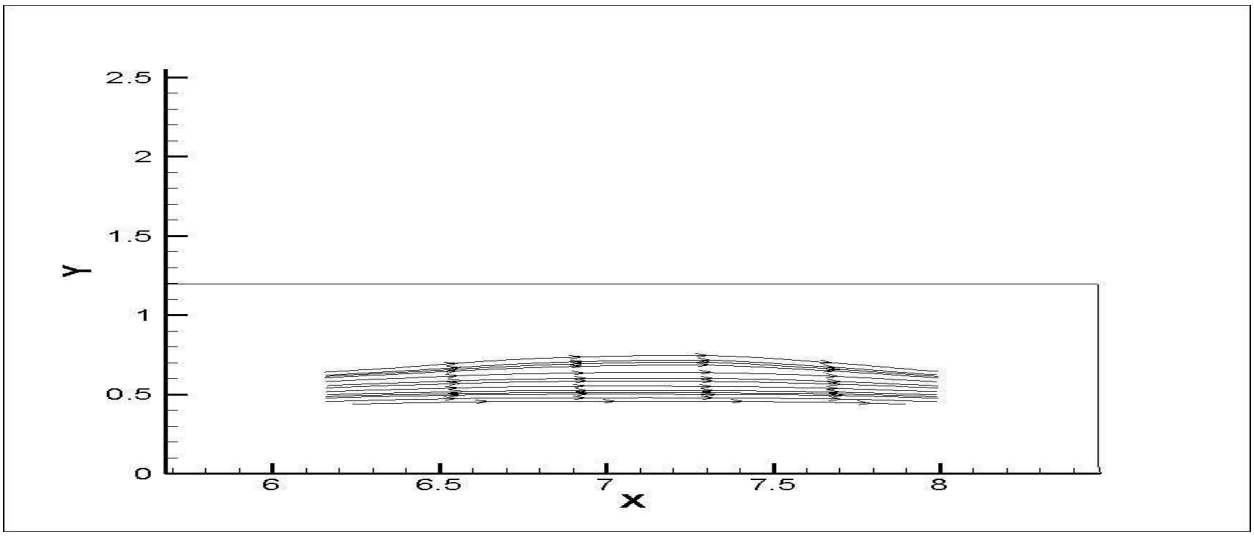

Figure 3.21: Pass line shown in Tecplot 360 (5-cm square test)

3.10 Compare with ADV data

After getting all of the data measured by LSPIV method, also use ADV method to measure the flow velocity data. Then use the ADV data compared with the LSPIV data, to make sure the LSPIV method is correct and real.

3.11 Additional parameters

Showing all the parameters can be important for interpreting the results. As every minor change in the parameters may influence the accuracy of the results, it is useful that every parameter used to obtain the velocity field should be specified.

3.11.1 Four-foot flume test

Here, the 5-cm square test is used as an example test. To make certain the 5-different seed particle size tests can be compared, it is important that all test variables are the same for the four tests. The following arrangement of variables and procedures was used:

- Benchmarks: See table 3.2
- Number of images: 250
- Time step= 0.033s
- Discharge: Q1 = 0.0722 m^3/s (2.55 cfs)
- Free-surface water level: Y1= 0.08 m
- Interrogation area (IA): 0.302 m (54 pix)
- Move discharge the center position J: DJ1 = 240-unit length
- Move discharge the center position I: DI1 = 84-unit length
- Distance from the top of the search area to the center: Sim1 = 60 pix
- Distance from the bottom of the search area to the center: Sip1 = 60 pix
- Distance from the upstream side of the search area to the center: Sjm1 = 60 pix
- Distance from the downstream side of the search area to the center: Sip1= 60 pix
- Grid point 1-2/3-4: 60
- Grid point 2-3/4-1: 20

- Velocity magnitude thresholds: V_t1= 0.001 to 3.0 m/s,
- Vx component magnitude thresholds: V_x1= 0.001 to 3.0 m/s
- Vy component magnitude thresholds: V_y1= -3.0 to 3.0 m/s

3.10.2 Tarbella flume channel test

For this series of tests, all of the variables differed from those used for the four-foot flume tests. Therefore, there was the need to create and set up a new variable test set. The LSPIV measurement procedure remained the same as for the four-ft flume, though. The changes reflect the use of the Tarbella flume. The following arrangement of variables and procedures were used for the Tarbela Flume:

Shallow depth Tarbella flume channel test

- Benchmarks: See table 3.3
- Number of images: 250
- Time step= 0.033s
- Discharge: Q2 = 2.464 m^3/s (87 cfs)
- Free-surface water level: Y2 = 0.8077 m
- Interrogation area (IA): 0.34 m (20 pix)
- Move discharge the center position J: DJ2 = 0-unit length
- Move discharge the center position I: DI2 = 0-unit length
- Distance from the top of the search area to the center: Sim2 = 30 pix
- Distance from the bottom of the search area to the center: Sip2 = 50 pix
- Distance from the upstream side of the search area to the center: Sjm2 = 50 pix
- Distance from the downstream side of the search area to the center: Sip2 = 50 pix

- Grid point 1-2/3-4: 20
- Grid point 2-3/4-1: 60
- Velocity magnitude thresholds: Vt2= 0.001 to 1.5 m/s,
- Vx component magnitude thresholds: Vx2= -1.5 to 1.5 m/s
- Vy component magnitude thresholds: Vy2= 0.001 to 1.5 m/s

Deep depth Tarbella flume channel test

- Benchmarks: See table 3.3
- Number of images: 250
- Time step= 0.033s
- Discharge: Q3 = 3.624 m^3/s (128 cfs)
- Free-surface water level: Y3 = 1.30 m
- Interrogation area (IA): 0.34 m (20 pix)
- Move discharge the center position J: DJ3 = 0-unit length
- Move discharge the center position I: DI3 = 0-unit length
- Distance from the top of the search area to the center: Sim3 = 50 pix
- Distance from the bottom of the search area to the center: Sip3 = 50 pix
- Distance from the upstream side of the search area to the center: Sjm3 = 50 pix
- Distance from the downstream side of the search area to the center: Sip3 = 50 pix
- Grid point 1-2/3-4: 20
- Grid point 2-3/4-1: 60
- Velocity magnitude thresholds: Vt3= 0.001 to 1.5 m/s,
- Vx component magnitude thresholds: Vx3= -1.5 to 1.5 m/s
- Vy component magnitude thresholds: Vy3= 0.001 to 1.5 m/s

CHAPTER 4, MEASUREMENT RESULTS AND ANALYSIS

4.1 Introduction

This chapter presents the results from the sets of experiments involving the two flumes. The first flume was used to investigate how tracer size may influence LSPIV accuracy in measuring flow velocity at water surfaces. The second flume, a much larger flume, was used with LSPIV to determine the flow field at a bendway weir subject to the scour of the sand bed upon which it was built. Of interest were the magnitude of the maximum velocity and how the flow field at a bendway weir varied with and without the presence of region of local scour.

4.2 Results from the four-foot flume channel

In the experiment using the 4-foot flume, five different sizes of tracers were used to investigate tracer size for LSPIV measurement. As noted in Chapter 3, they were 0.7cm circle (C-0.7), 1cm square (S-1), 3cm square (S-3), 5cm square (S-5), and 10cm square (S-10); the acronyms mentioned are used subsequently in this chapter to describe the performances of the LSPIV tracers for the particular flow field.

Figures 4.2a-j show images of each test process with the tracers in use, and then present the velocity results determined using the steps involved in the LSPIV method described in Chapter 3.

(a)

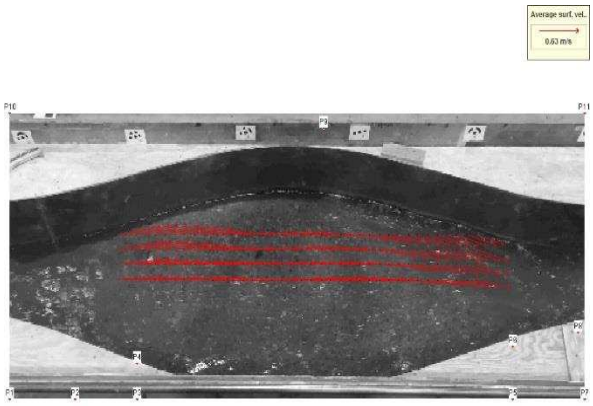
Average surf. vel.
0.63 m/s

(b)

(c)

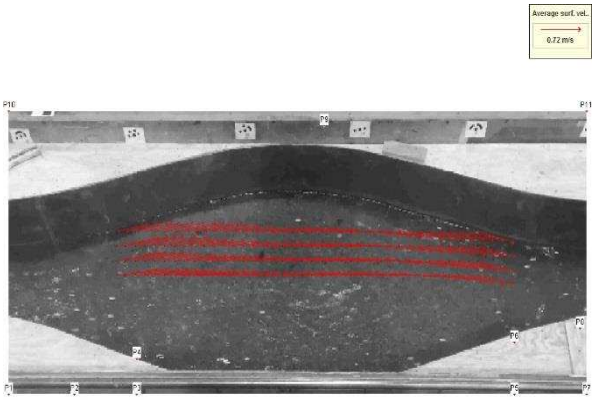
Average surf. vel.
0.72 m/s

(d)

(e)

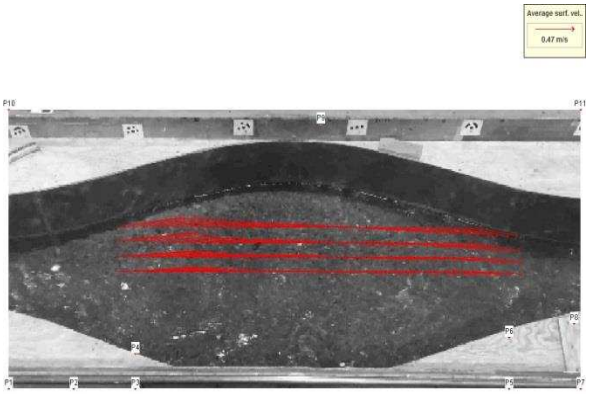
Average surf. vel.
0.47 m/s

(f)

(g)

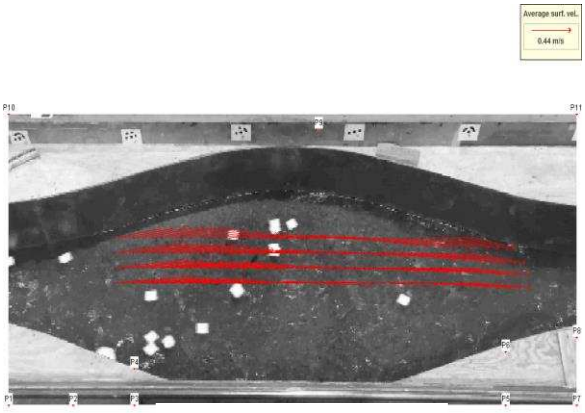

(h)

(i)

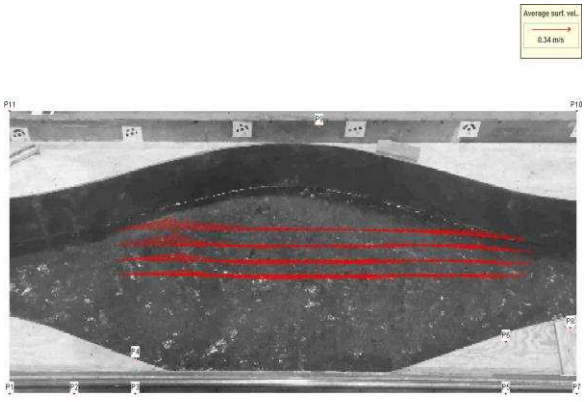

(j)

Figure 4.1: Presented here are ten images showing flow in the contraction-expansion sequence set in the 4-foot flume channel test process. Also shown are the velocity results obtained with the tracers: (a) C-0.7 test process, (b) C-0.7 velocity result, (c) S-1 test process, (d) S-1 velocity result, (e) S-3 test process, (f) S-3 velocity result, (g) S-5 test process, (h) S-5 velocity result, (i) S-10 test process, (j) S-10 velocity result

However, on closer viewing, some differences are evident. In the tests involving the three larger tracer sizes, S-3, S-5 and S-10, the tracers dispersed with the flow. But, for tests C-0.7 and S-1, some tracers became bunched together and behaved as drifting clumps, whose overall tracer size was considerably bigger than that of an individual tracer particle. This clumping effect is due to the effect of surface tension causing individual particles essentially to stick together. Figures 4.2a&b show two photographs of clumped tracers. In Figure 4.2a there are about five to eight 0.7cm-diameter tracer particles collected together. Consequently, the "effective" tracer size was about 3.5 to 5.6cm. Also, in Figure 4.2b, are about three to four 1cm-square tracer particles collected together. In this example, the consequent effective tracer size was about 3 to 4cm wide. This clumping of tracers did not happen at every place on the water surface, but it happened in some places, forming about three to eight clumps in an image. This clumping can be shown to have affected the values of water-surface velocity obtained with the LSPIV method, because the software averaged the velocities obtained from the tracers moving through points on the grid. On the whole, the larger tracers tended to drift a bit slower than the local water flow at a point. The velocity data were calculated by means of the Fudda LSPIV software described in Chapter 3.

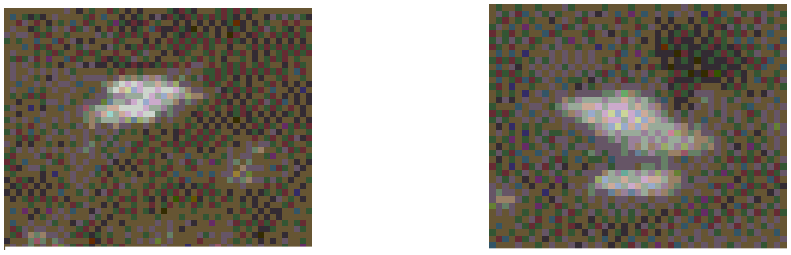

(a) (b)

Figure 4.2: Photographs of bunched tracers. (a) in the C-0.7 test (b) in the S-1 test. The photographs are enlarged from actual LSPIV images

A first task was to compare the minimum and maximum values of velocities obtained from each of these 5 tests. The spreadsheet system Excel was used to calculate these results. Table 4.1 shows the minimum velocities, maximum velocities and where they occurred. In this table, x and y are coordinate, V_x is the velocity in the x direction, V_y is the velocity in the y direction, and V_T is the total velocity.

Table 4.1: Velocity comparisons and occurrence locations

	x (m)	y(m)	V_X (m/s)	V_Y (m/s)	V_T (m/s)
C-0.7					
Max	6.296	0.504	0.744	0.0116	0.74409
Min	7.1976	0.6888	0.2995	0.0106	0.29969
S-1					
Max	6.2008	0.5656	0.7938	0.1238	0.8034
Min	6.912	0.504	0.4364	0.0323	0.43759
S-3					
Max	6.2008	0.504	0.9105	0.0358	0.9112
Min	7.668	0.5656	0.482	-0.0244	0.48262
S-5					
Max	6.2008	0.504	0.8403	0.0596	0.84241
Min	6.7664	0.6888	0.4194	0.0415	0.42145
S-10					
Max	6.2456	0.504	0.668	0.0161	0.66819
Min	6.912	0.6944	0.2872	0.0089	0.28734

In this table, it can be seen that the maximum velocities are nearly the same for tests S-1, S-3, S-5 and C-0.7; i.e. for the four tests with the larger tracers. But, for the S-10 test, the maximum velocity is smaller in value than those obtained for the other tests. The values of minimum velocities are nearly the same for the three tests S-1, S-3 and S-5. The minimum velocities are smaller than the other three minimum velocities in S-10 and C-0.7 test. Additionally, it is useful to compare the values of the velocity on the x direction, the velocity on

the y direction, and the total velocity. For this purpose, twenty points were selected. The twenty points are shown in Table 4.2, and Figure 4.3 displays the velocity values compared for the x direction, the y direction, and the total velocity.

Table 4.2: Locations of the twenty selected points

NO.	X	Y	NO.	X	Y
1	6.2008	0.504	11	6.2008	0.6272
2	6.6264	0.504	12	6.6264	0.6272
3	7.1024	0.504	13	7.1024	0.6272
4	7.528	0.504	14	7.528	0.6272
5	7.9536	0.504	15	7.9536	0.6272
6	6.2008	0.5656	16	6.2008	0.6888
7	6.6264	0.5656	17	6.6264	0.6888
8	7.1024	0.5656	18	7.1024	0.6888
9	7.528	0.5656	19	7.528	0.6888
10	7.9536	0.5656	20	7.9536	0.6888

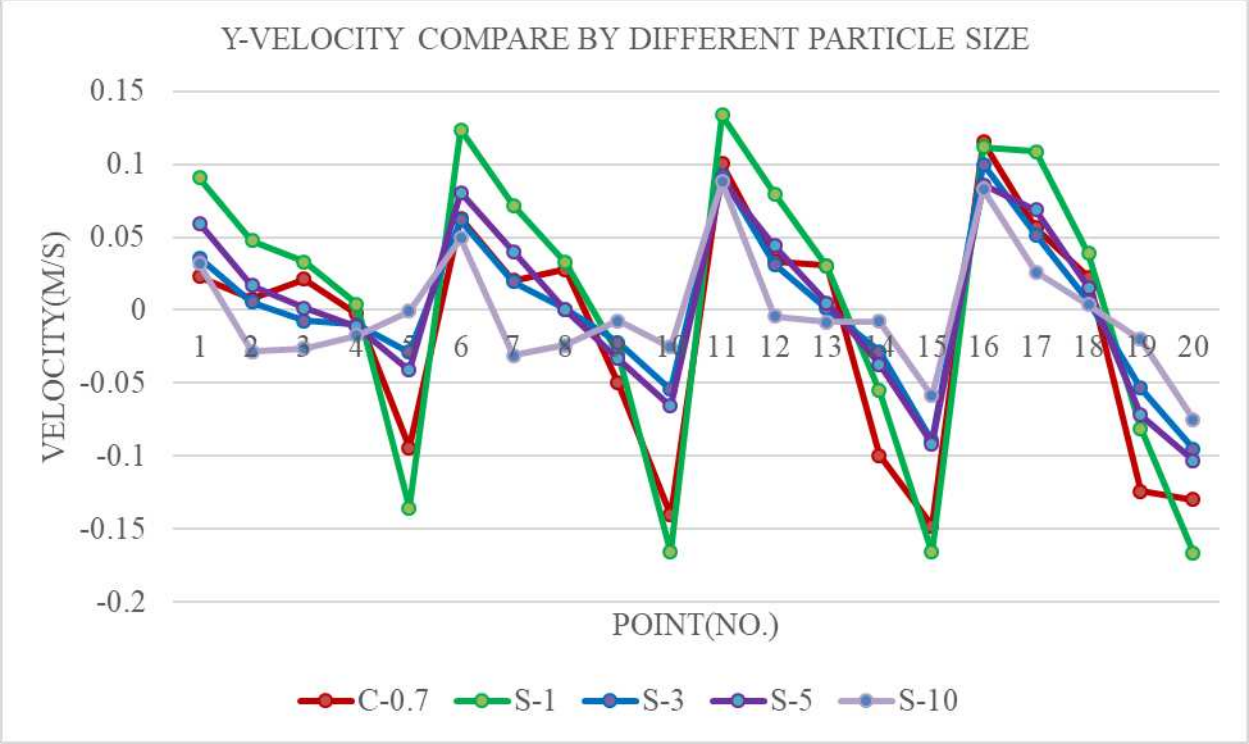
Y-VELOCITY COMPARE BY DIFFERENT PARTICLE SIZE
VELOCITY(M/S)
0.15
0.1
0.05
0
-0.05
-0.1
-0.15
-0.2
1 2 3 4 5 6 7 8 9 10 11 12 13 14 15 16 17 18 19 20
POINT(NO.)
C-0.7
S-1
S-3
S-5
S-10

(a)

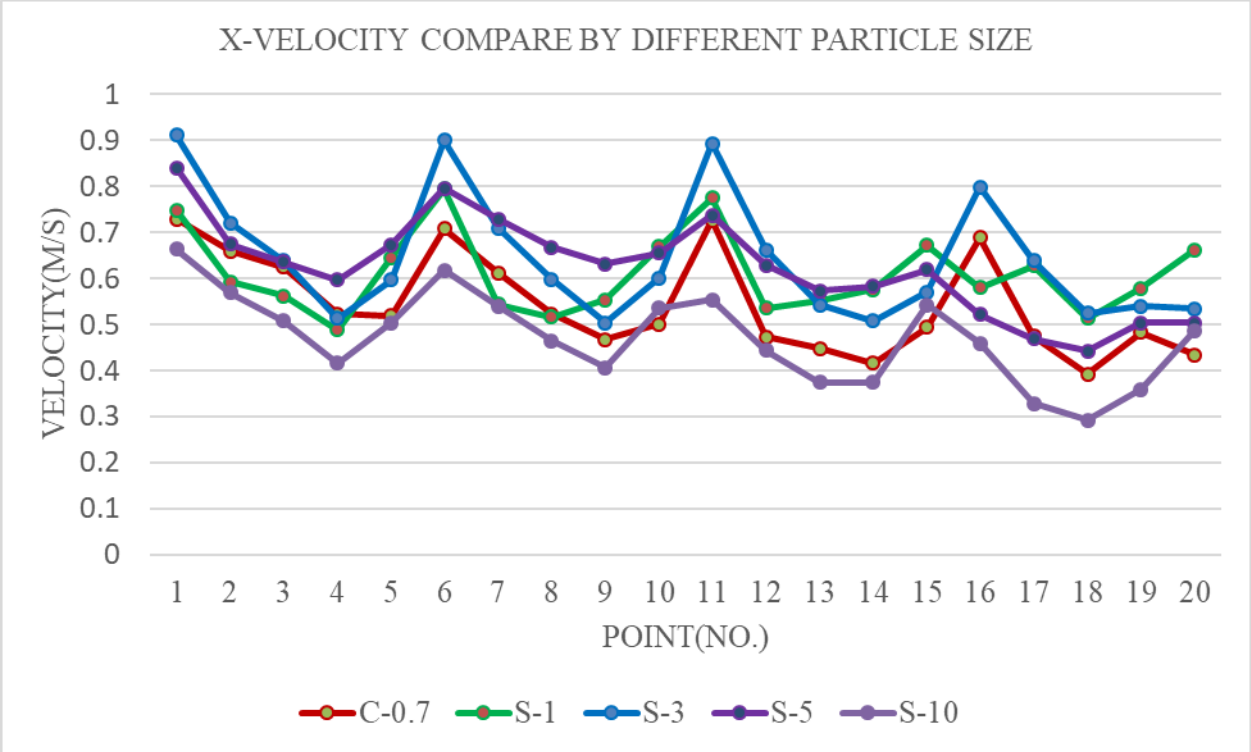
X-VELOCITY COMPARE BY DIFFERENT PARTICLE SIZE
VELOCITY(M/S)
1
0.9
0.8
0.7
0.6
0.5
0.4
0.3
0.2
0.1
0
1 2 3 4 5 6 7 8 9 10 11 12 13 14 15 16 17 18 19 20
POINT(NO.)
C-0.7
S-1
S-3
S-5
S-10

(b)

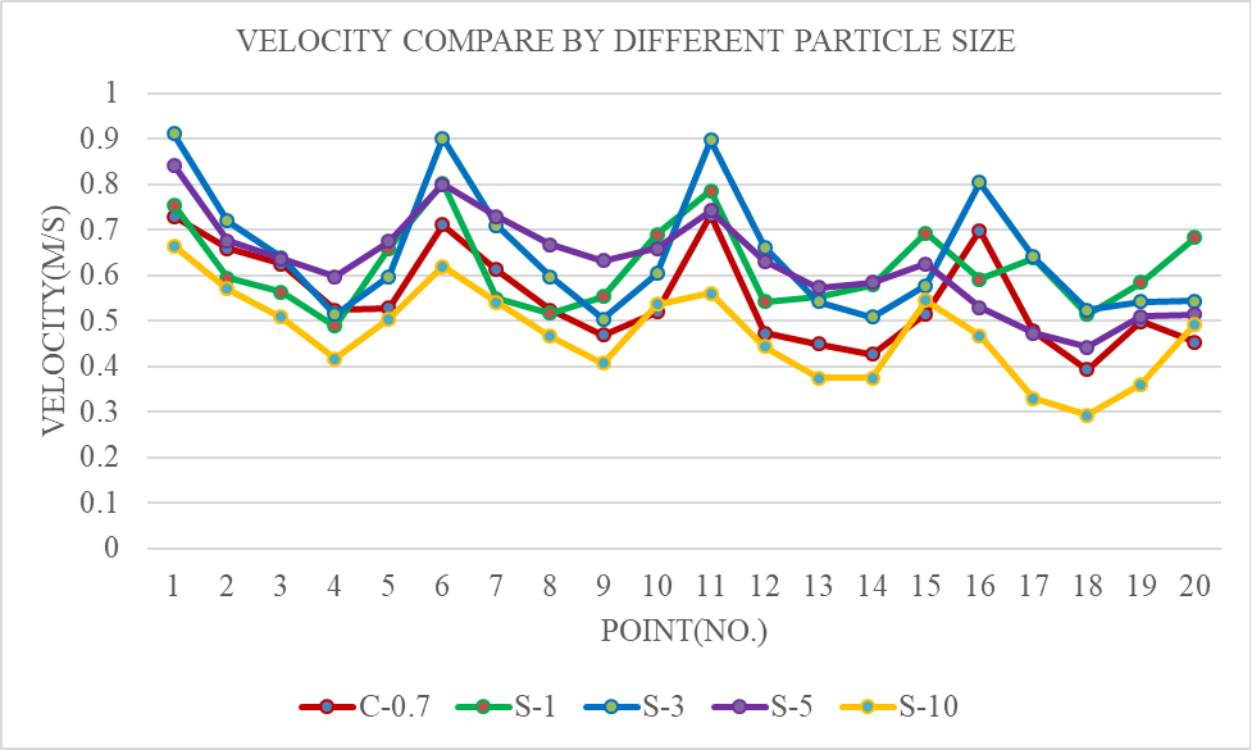

(c)

Figure 4.3: Comparisons of velocities obtained for the various sizes of tracer: (a) the velocity along the x direction; (b) velocity along the y direction; and, (c) the total velocity

For the three charts given in Figures 4.2a-c, the red line refers to test C-0.7 data; the green line refers to test S-1 data; the blue line refers to test S-3 test data; the purple line refers to teste S-5 test data; and, the yellow line refers to test S-10 test data. The yellow line is clearly below the other lines in these three charts. Also, the red is next lower than the other lines. These results mean that the test data on S-10 test are usually even almost completely smaller than other test data, and the test data on C-0.7 test and S-1 test data are always smaller than other test data. This set of comparisons shows that the 3cm square, 5cm square three sizes are suitable tracers for the size of the flow field; i.e., the D/d value is suitable to reflect the changes in flow velocity and flow patterns. However, the 10cm square is too large to use as the tracer for this flow field.

Also, the 0.7cm circle and 1cm square are not appropriate sizes for use as tracers formed of paper, because of the bunching problem described above.

From the charts presented in Figure 4.3a-c, it is possible to show the extent to which the average velocity of flow at locations in the flow field varied with tracer size. Figure 4.4 compares the average velocity at a location with the length dimension of each tracer. And also is included to compare the tracer sizes in these five different tests. Note that, because transverse velocity was small at this location, the data for V_X coincide essentially with the data for V_T.

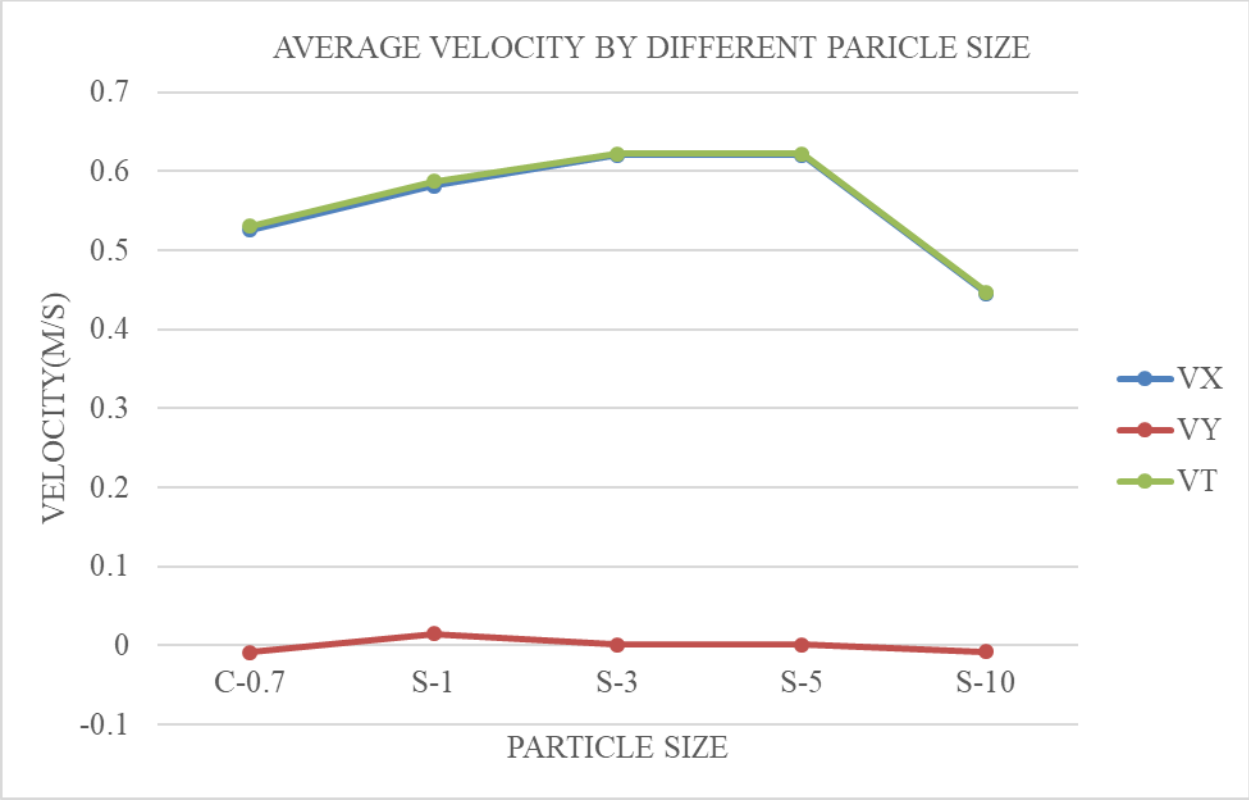

Figure 4.4: Average velocity by varied tracer size

Table 4.3: Tracer size

	Length of side or diameter (cm)	Perimeter (cm)	Area (cm^2)
C-0.7	0.7	2.2	0.39
S-1	1	4	1.0
S-3	3	12	9.0
S-5	5	20	25.0
S-10	10	40	100.0

In Figure 4.4, it can be seen that the velocities in the y-direction are estimated as being negative when the tracer length was 0.7cm and 10cm. The negative values relate to the size of the tracers, especially the fact that the smallest tracers bunched to form a tracer similar in size to the largest tracer. The size of the tracers tended to cause the bunched and the largest tracers to slightly drift, thereby indicating a negative velocity. In general, the velocity in the y-direction was negligibly small, so that it did not influence the total velocity. The trend in Figure 4.2 indicates that the 0.7cm circle, 1cm square and 10cm square do not act as effective, accurate tracers for this flow field; they give lower values of total velocity than do the other tracers. Figure 4.3 and Figure 4.4 show the U (velocity on the X direction) and V (velocity on the Y direction) contour when use varied size tracers.

In Figure 4.5, shown are the U contours obtained when variable-sized tracers were used. The red area means that this location has relatively high velocity, and the blue area means this location has relatively low velocity. Comparison of these five different velocity contours indicates that for the larger areas high velocity happens on the S-1, S-3 and S-5 tests. However, on the S-10 tests, the flow velocities are nearly the same on every place. Based on basic concepts of fluid mechanics continuity, it is evident that the regions of high velocity happen in the contraction condition, and that the areas of low velocity happen in the expansion condition.

These results suggest that the S-1, S-3 and S-5 tests produce the most accuracy of the five tests. At first, the channel expands along the 6m-7.2m area. And the high velocity happens at the start of the channel, because after that the channel expands and the flow slows a bit; the velocity reduces because the channel shape widens. Then the channel contracts along the 7.2m-8m region. Also, S-1, S-3 and S-5 tests show the contraction effect accurately. But the C-0.7 and S-10 tests do not produce sufficient information detail to show the velocity variation.

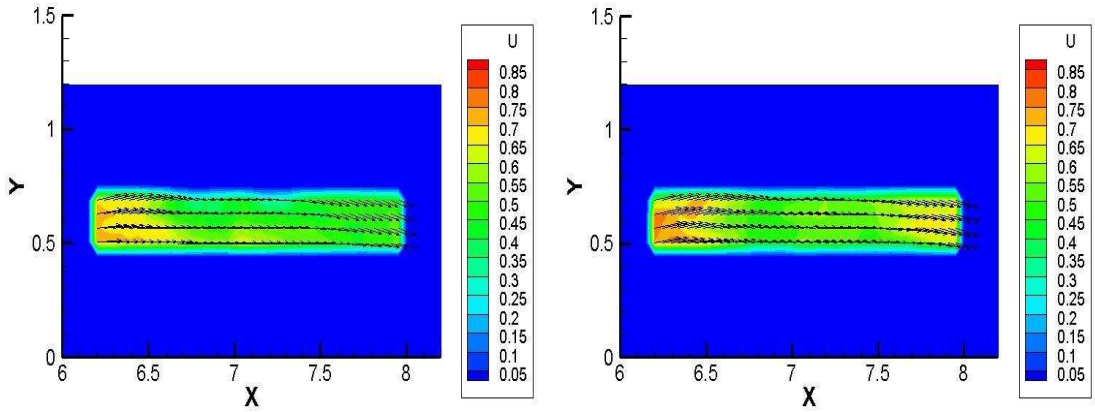

(a) (b)

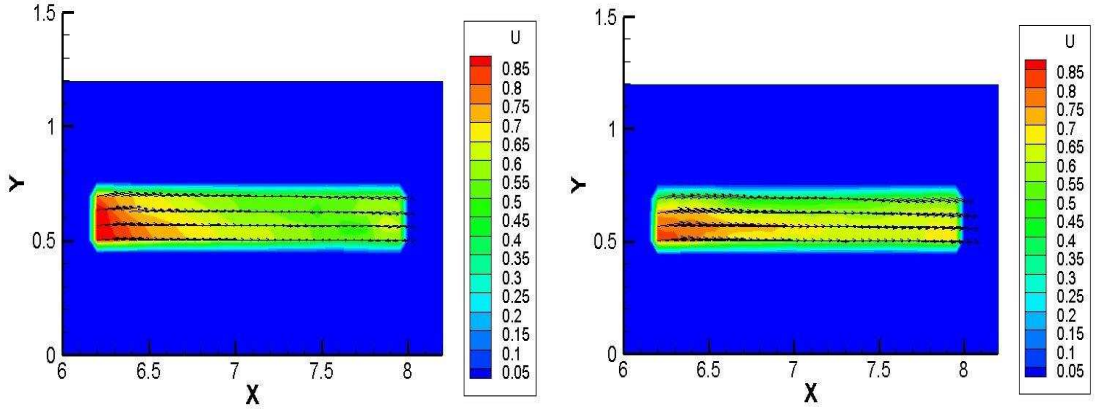

(c) (d)

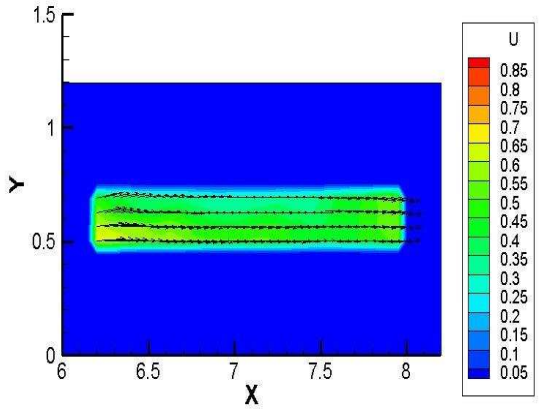

(e)

Remarks (unit):

X: m

Y: m

U: m/s

Figure 4.5: Shown here are the U contours estimated using varied size tracers, (a) C-0.7, (b) S-1, (c) S-3, (d) S-5, (e) S-10

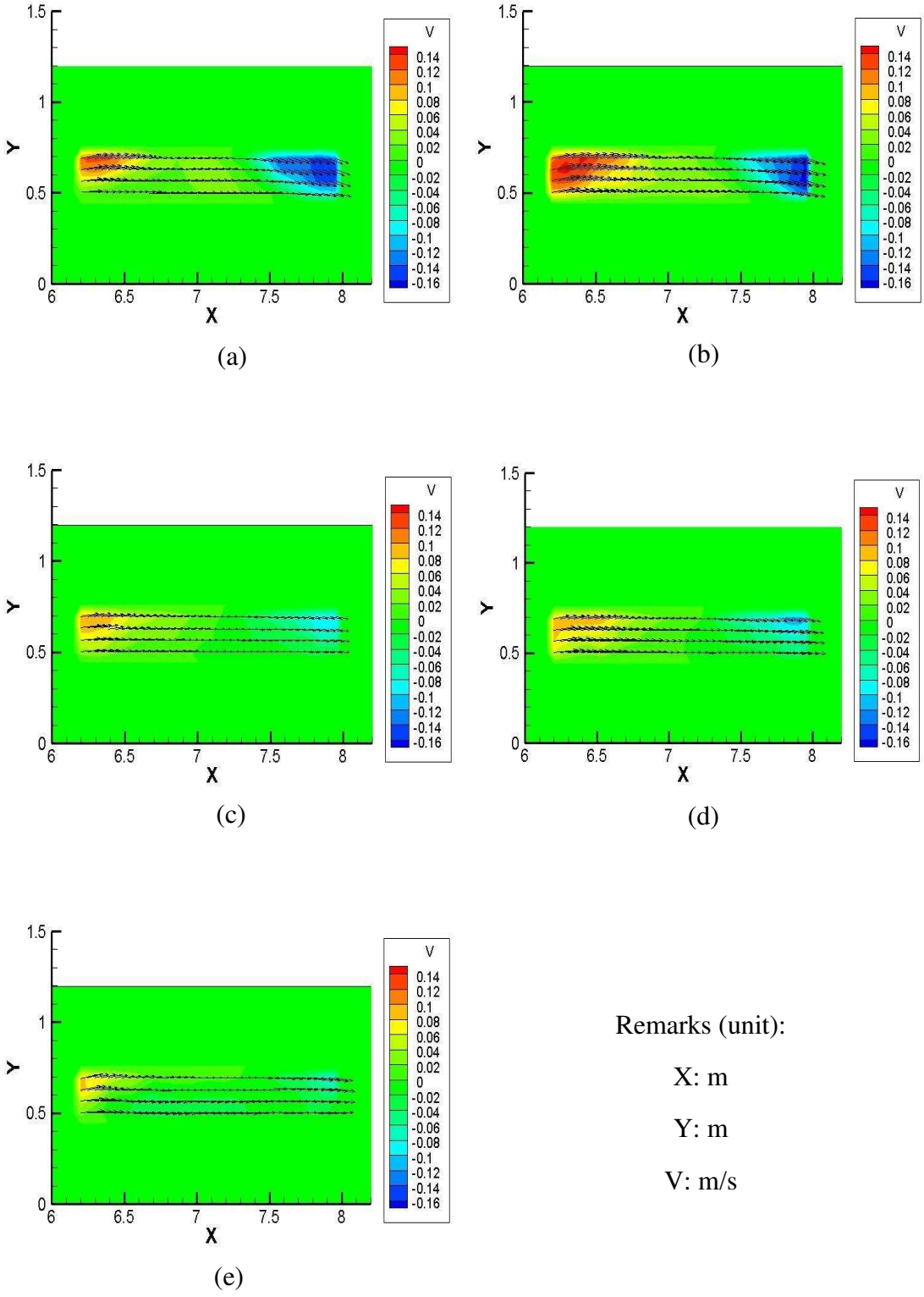

Figure 4.6: Shown here are V contours obtained with varied size tracers, (a) C-0.7, (b) S-1, (c) S-3, (d) S-5, (e) S-10

In Figure 4.6, there also are V contours resulting with the varied size tracers. The smallest area low velocity and high velocity all happen on the S-10 test much differently than V contours. This finding proves again that the 10cm square tracer was unsuitable as a tracer for this experiment. For the other four tests, all manifest that the channel is contracting along the 6 to 7.2m length and then expanding along the 7.2 to 8m length. But on the C-0.7 and S-1, they have too big positive direction velocity and negative direction velocity. They are too big will not happen this condition channel. And S-3 and S-5 are the best results on these tests.

The last activity was to compare the path-line images determined from these five tests. Because the velocity data on these five tests were very similar and the velocity directions were correctly identified for every test, therefore the path line images were nearly the same on these

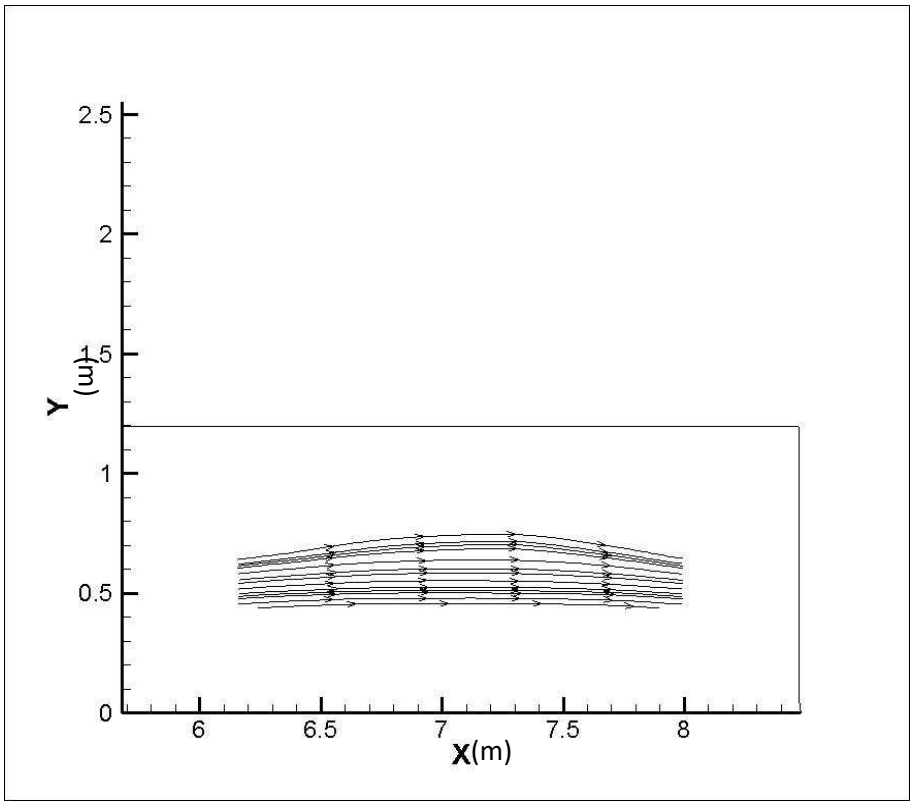

Figure 4.7: Path line image for the S-5 test

tests. Therefore, it was convenient here to show only the path line which is the S-5 test, as illustrated in Figure 4.7.

To summarize the findings, it can be readily shown that the 10cm square cannot be used as a tracer for this experiment, because it is too big and thus influences the test results. There are many factors that make a tracer unsuitable for use in LSPIV measurement: tracer mass, tracer area, flow resistance, surface tension, and the effects of major turbulence and wind. Also, the 0.7cm circle and 1cm square were so not optimal tracers, because they were too small, stuck together, and therefore influenced the velocity data. And the collection profile will happen to influence the results. Then, it can be confirmed that 3cm square and 5cm square were the best tracer sizes. These sizes can make the results more accurate and integrated. Based on this project, the maximum width of the channel is about 1.14 m and minimum width of the channel is about 0.44 m. If the average width of the channel is about 0.79 m, the tracer size is about from 3.80% to 6.33% of the width of the channel. This tracer size range is the best for use in the LSPIV method.

4.3 Tarbella flume channel results and analysis

This section discusses the flow field around and over the bendway weir shown in Figure 3.6 and explores how LSPIV can be used to determine how the flow field changes as scour develops locally around the bendway weir.

4.3.1 Shallow depth Tarbella flume channel test

The process began, as mentioned above (see Figure 4.8), by first using the Fudaa-LSPIV software to calculate velocities populating the free-surface flow velocity. As in Figure 4.8, use was made of the blue imaginary line to organize the total zone into four different zones. The “A”

zone is the flow before going over and around the bendway weir. The “B” zone is over the bendway weir. The “C” zone is the flow after having gone over the bendway weir and downstream of the bendway weir way. And, the “D” zone is the flow near the flume’s west sidewall. Then the velocity flow field and the changes it experienced, especially near the sidewall. In zone “A,” the velocity direction goes along the flume and did not have an evident bendway weir effect. In this zone, the velocity was bigger than in the approach-flow region upstream. The location of the maximum velocity occurred at the yellow star shown in Figure 4.8, which did not reach the bendway weir but was close to it. After the bendway weir, the velocity is a little lower than the maximum velocity. In the left part of the “B” zone, the velocity was much smaller than before because of the presence of the bendway weir. In the “C” zone, the velocity

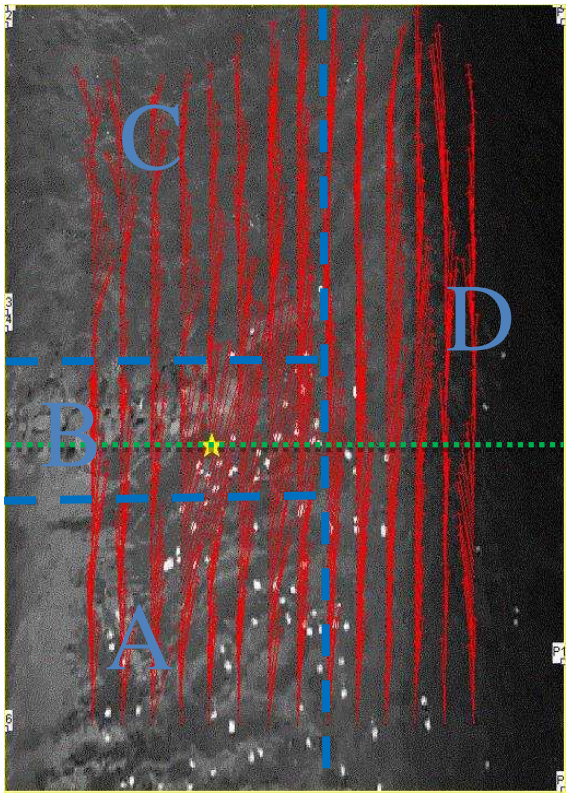

Figure 4.8: Free-surface flow velocity in shallow depth test

changed considerably, because the flow entered the wake region downstream of the bendway weir. The direction of the velocity was not uniform or orderly. On right of the "D" zone, before going over the bendway weir, the velocity direction was changed by the bendway weir. But after going past the bendway weir, the direction of flow changed to the opposite direction. Through the last part of the "D" zone, the flow experienced some waviness and large turbulence attributable to dunes formed of eroded sand removed from the sediment recess. Figure 4.9 illustrates the distribution of flow velocity across the axis of the bendway weir. This figure

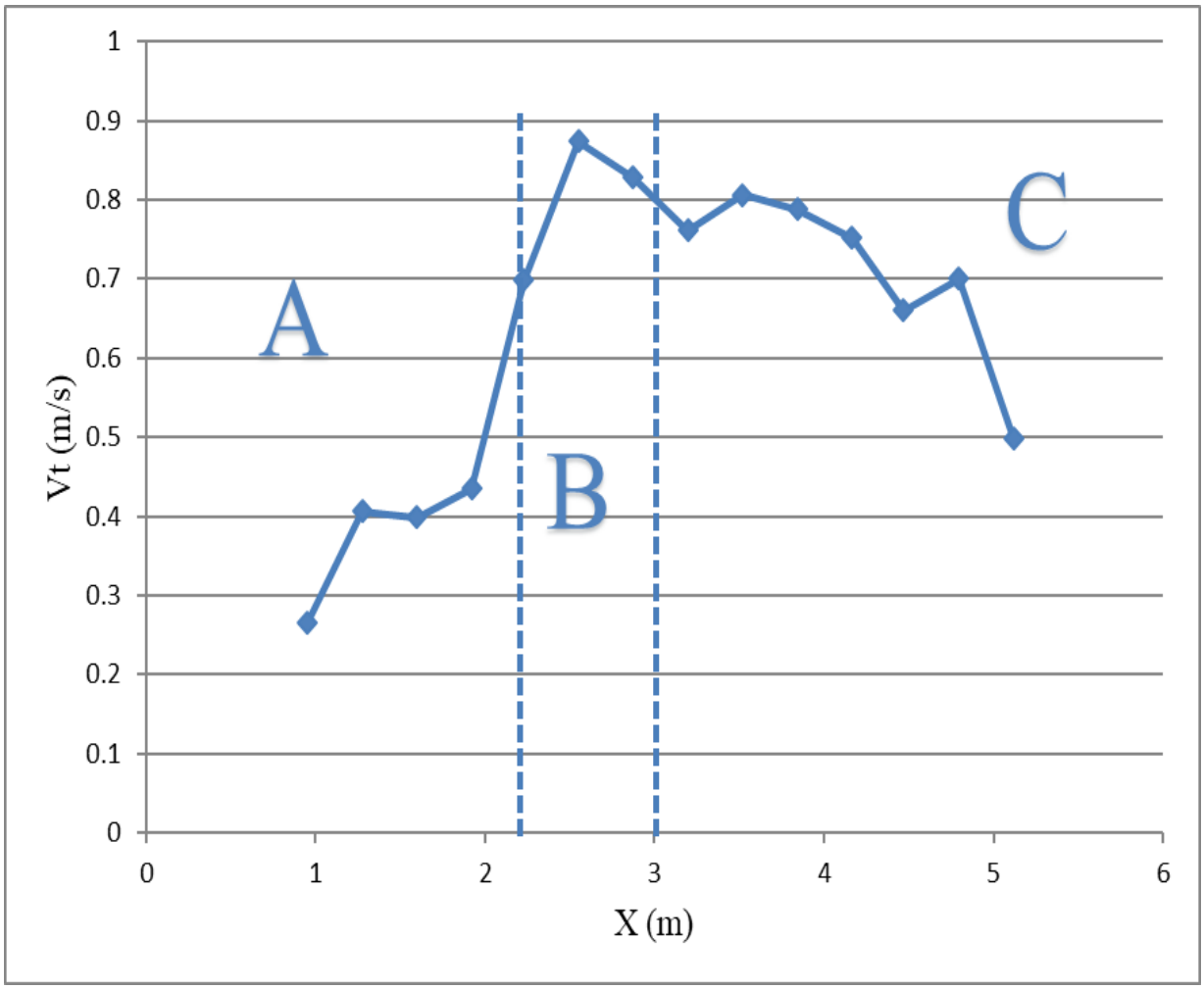

Figure 4.9: Total velocity analysis when on the bendway weir (Y= 15.783) on the deep flow test

shows that the velocity was greatest around the end of the bendway weir. The maximum velocity at the end of the bendway weir was 0.264ft/s (0.88m/s). The dashed lines indicate the end of the bendway weir.

In Figure 4.9, use the blue imaginary line cut through three zones. On the left side of the maximum velocity is zone “A,” which also extends over the bendway weir. The velocities are much smaller than the maximum velocity on zone “A”. But the other side velocities are just a little smaller than the maximum velocity until near the side wall on the zone “B”. This means the rock can much reduce the velocity when the flow goes through it.

The next step in the analysis required using Tecplot 360 software to create the image indicating values of the U contour, V contour and path line associated with this flow field. The U contours and V contours are shown in Figure 4.10.

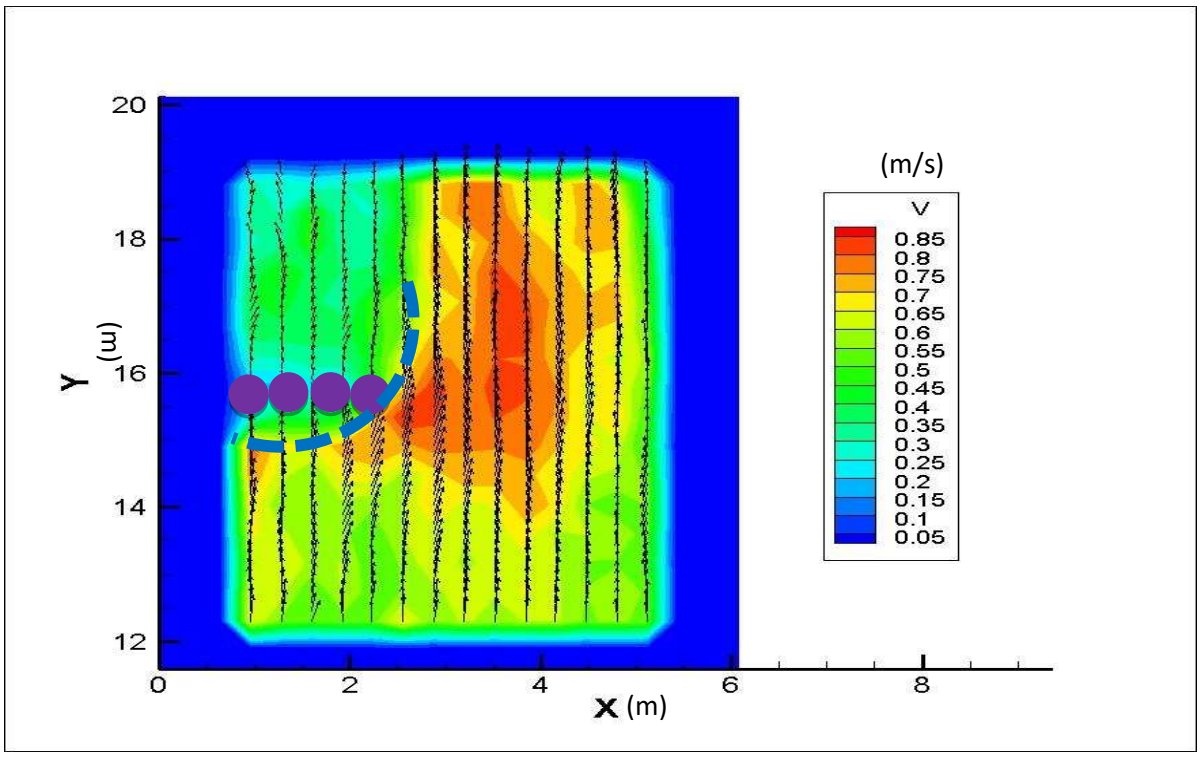

(a)

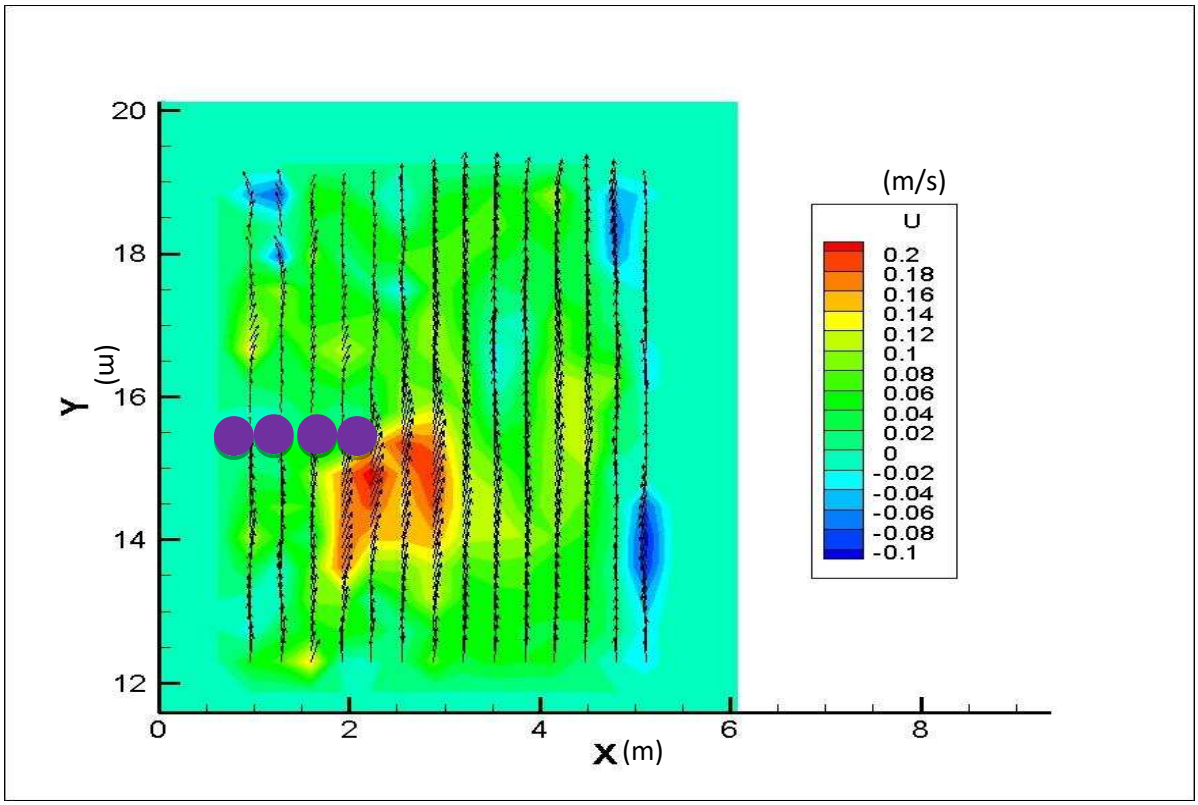

(b)

Figure 4.10: Velocity contour in shallow depth test, (a) V contour (b) U contour

In Figure 4.10 (a), use of the purple circle means the sidewall. In the V contour, the red area means this place has high velocity, and green area means this place has low velocity. First, it can draw a blue imaginary curve line to cut this contour image. On the right of the curve the place has high velocity. And on another side, the velocity is lower than other side. In other words, the sidewall changes the velocity. Before going through the sidewall, the flow has high velocity. After going through the sidewall, the energy is expended. Therefore, the flow velocity becomes lower.

In Figure 4.10 (b), the red are means this place has positive (right) direction velocity and blue area means this place has negative (left) direction velocity. Also, the maximum value positive velocity happened at the part place of the maximum velocity on the Figure (a). This means sidewall will change the flow direction directly and immediately. And after that, the change will return quickly. There are about four places that have negative velocity.

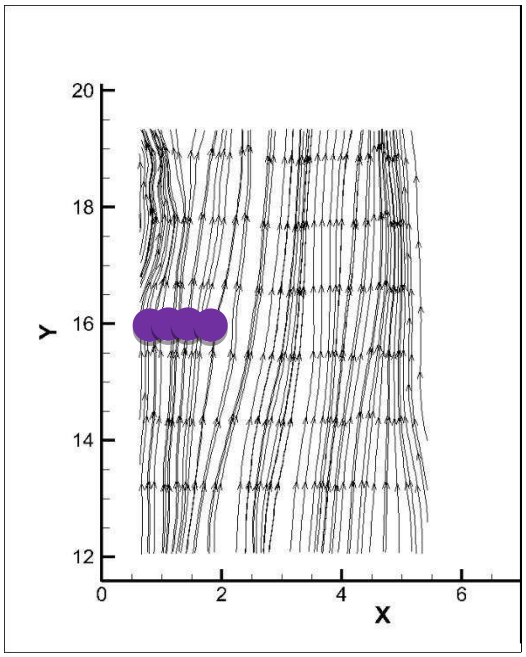

Figure 4.11: Path of flow line in shallow depth test

The observed path lines for this flow are shown in Figure 4.11.The four purple circles in this figure indicate the bendway weir. Based on the flow pathlines shown in this image, it can be seen that the flow swings largely around the bendway weir, with some flow passing over the bendway weir. After going over the bendway weir, the flow path-lines become more irregular, because they have some strange profiles. These are all of the profile flows that show the flow going through the sidewall.

4.3.2 Deep depth Tarbella flume channel test

For the bendway weir in deep flow, the process for determining the flow field was the same as for the bendway weir in shallow flow. The software Fudaa LSPIV was used to calculate the flow velocities at the free-surface, as outlined in Figure 4.12.

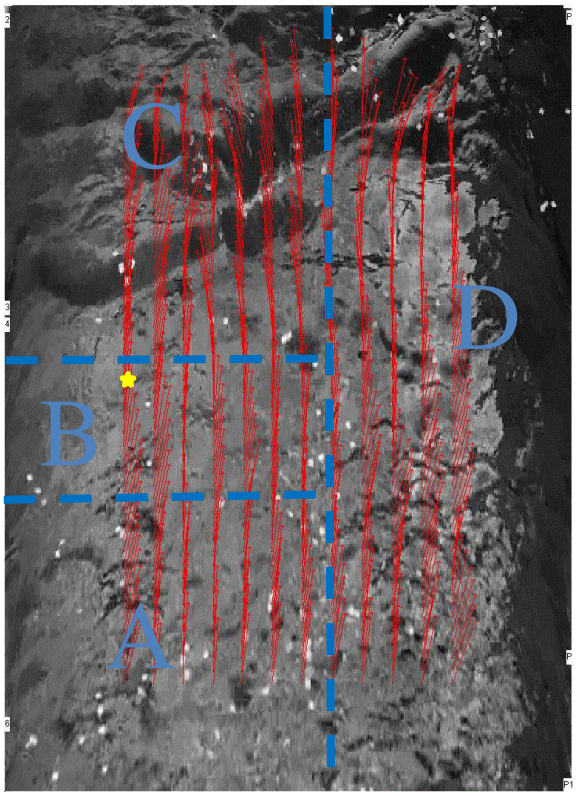

Figure 4.12: Free-surface flow velocity in shallow depth test

The same system was used to mark and delineate the IA and search areas. This step soon showed the flow field to have substantial differences compared with the flow field for the bendway weir in the shallow flow case. The maximum velocity coincided with the location of the yellow star indicated in Figure 4.12. The location was slightly downstream of the crest of the bendway weir. The value is about 0.8724m/s. Also, it was somewhat less that the maximum determined for the shallow flow case. In the "D" zone, the flow velocities all are directed downstream. Additionally, in the "A" and "B" zones, the velocities are smaller, but they also go in the downstream direction. Only on the "C" zone, do the velocities become rather irregular, or seemingly so. The flow velocities change very quickly and do not seem to follow any

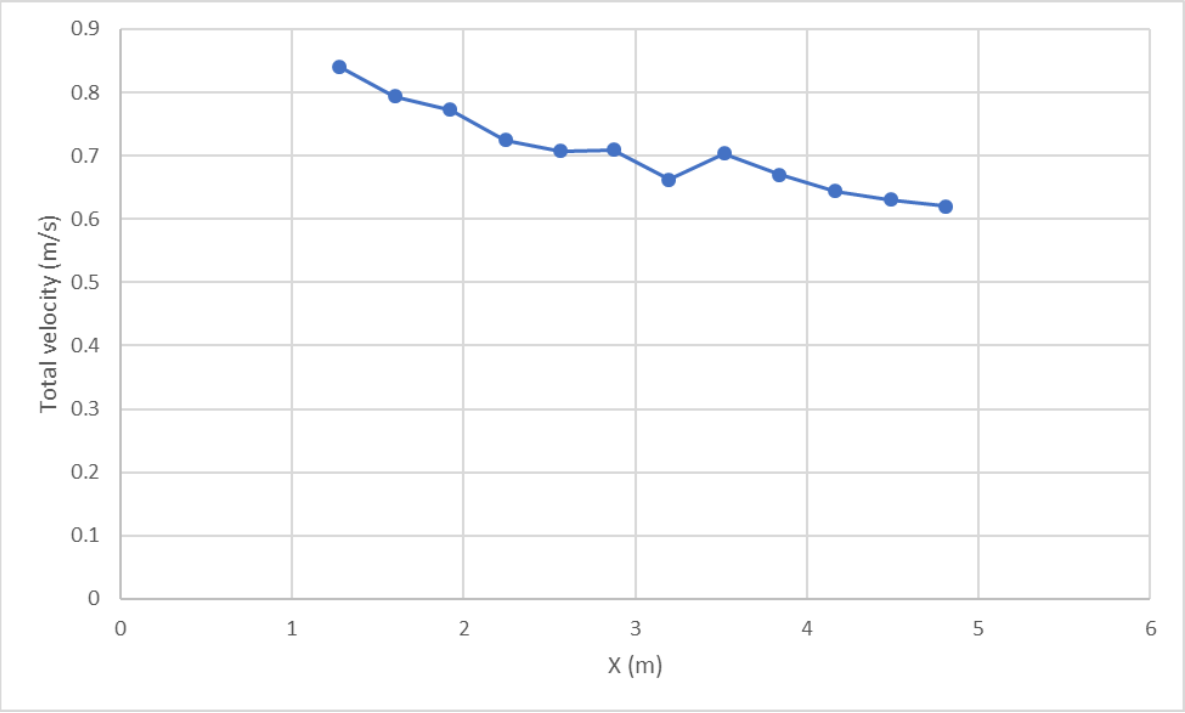

Figure 4.13: Total velocity analysis when on the bendway weir (Y= 15.783) on the deep flow test distribution.

The next force on the total velocities on the bendway weir are shown in Figure 4.13. Based on the figure that can be found, the total velocity descends when the X moves from small to big, and when the velocity is suddenly falling and rising on the end of the bendway weir.

Figure 4.14 shows the velocities presented in the Tecplot 360 software. This figure also presents values of streamwise and transverse velocities presented in terms of U contours, V contours and flow path-lines fort this flow.

In Figure 4.14, the velocity scale is the same as in the Figure 4.10. In Figure 4.14 (a), the high velocity area concentrates near the bendway weir. Other aspects of the flow contours are nearly the same as for the deep flow case (Figure 4.10). A small change is that the flow velocities were bigger after going over the sidewall, because the wake region was not so definite as in the shallow flow case. In Figure 4.14 (b), the velocities are directed downstream along the outer four path-lines. However, in the center region of the flow, after going over the bendway weir, the flow velocities tend to the left direction (looking downstream). The LSPIV method usefully illuminates the differences in the flow fields between the shallow- and deep-water cases.

The use of the Tecplot 360 software created the path-lines of flow as shown in Figure 4.15. In this figure, it is evident that more contraction flow occurred after the flow went over the sidewall. Also, more expansion of flow occurred before going over the sidewall. Here, the LSPIV shows how the flow responded to the presence of the bendway weir.

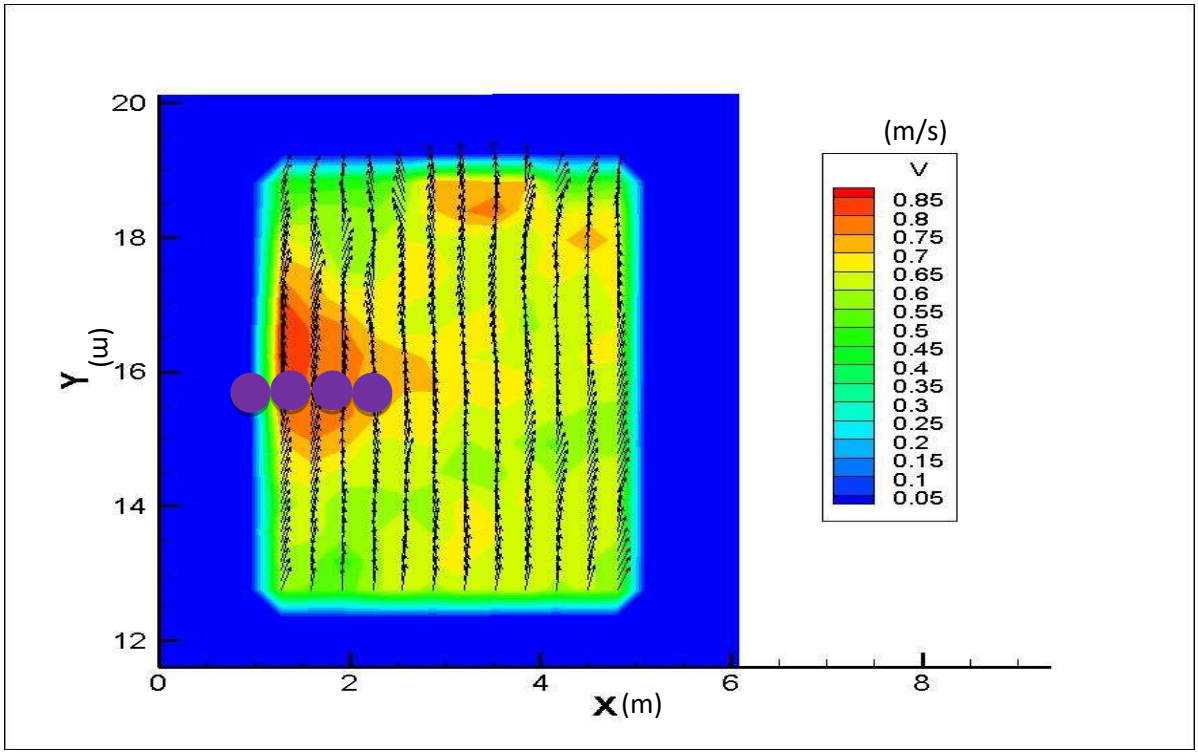

(a)

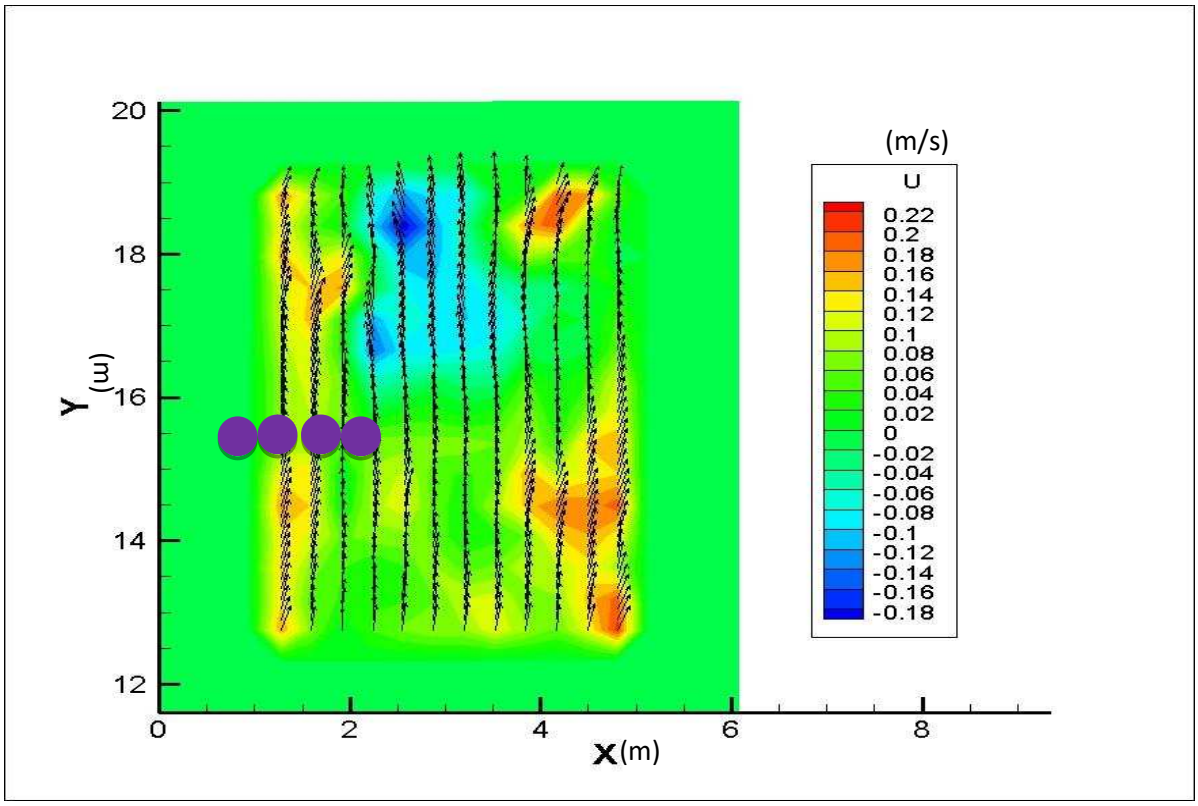

(b)

Figure 4.14: Velocity contour in deep depth test, (a) V contours (b) U contours

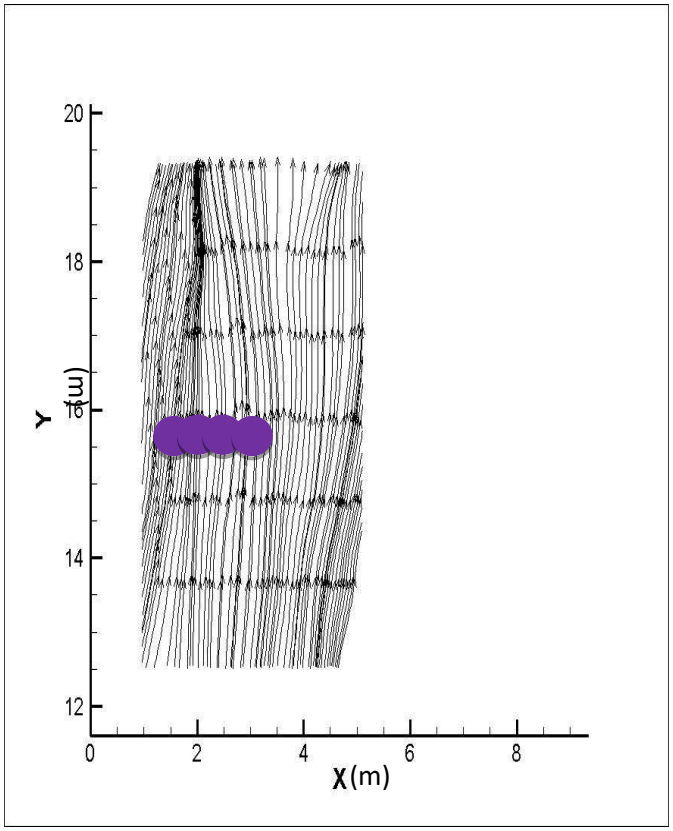

Figure 4.15: Path of flow lines in the shallow depth test

4.3.3 The utility of the LSPIV method

Using the LSPIV measurements to calculate the flow velocities, it becomes readily evident that there are major differences in flow field over the bendway weir when the depth is shallow and deep relative to the height of the bendway weir. Quite a few differences are evident and affect the magnitude of flow velocity near the end of the bendway weir. It can also be demonstrated that the LSPIV method is useful comparing on the different flow conditions. Therefore, the LSPIV method holds much promise for use in similar types of experiments, both in the laboratory and in the field.

4.4 Using the ADV method compared to the LSPIV method

For making right the data measured by LSPIV method, use the ADV method to measure the same condition. Figure 4.16 shows the maximum velocity (blue line), mean velocity (black line) and minimum velocity (red line) change by depth on the point where X=7.43, Y =0.63. In Figure 4.16, it can be found that themaximum velocity and minimum velocity change quickly and irregularly. And mean velocity is reduced base on the depth increase. From the LSPIV velocity data, choose the nearest this point (7.43, 0.63), to get the table 4.4.

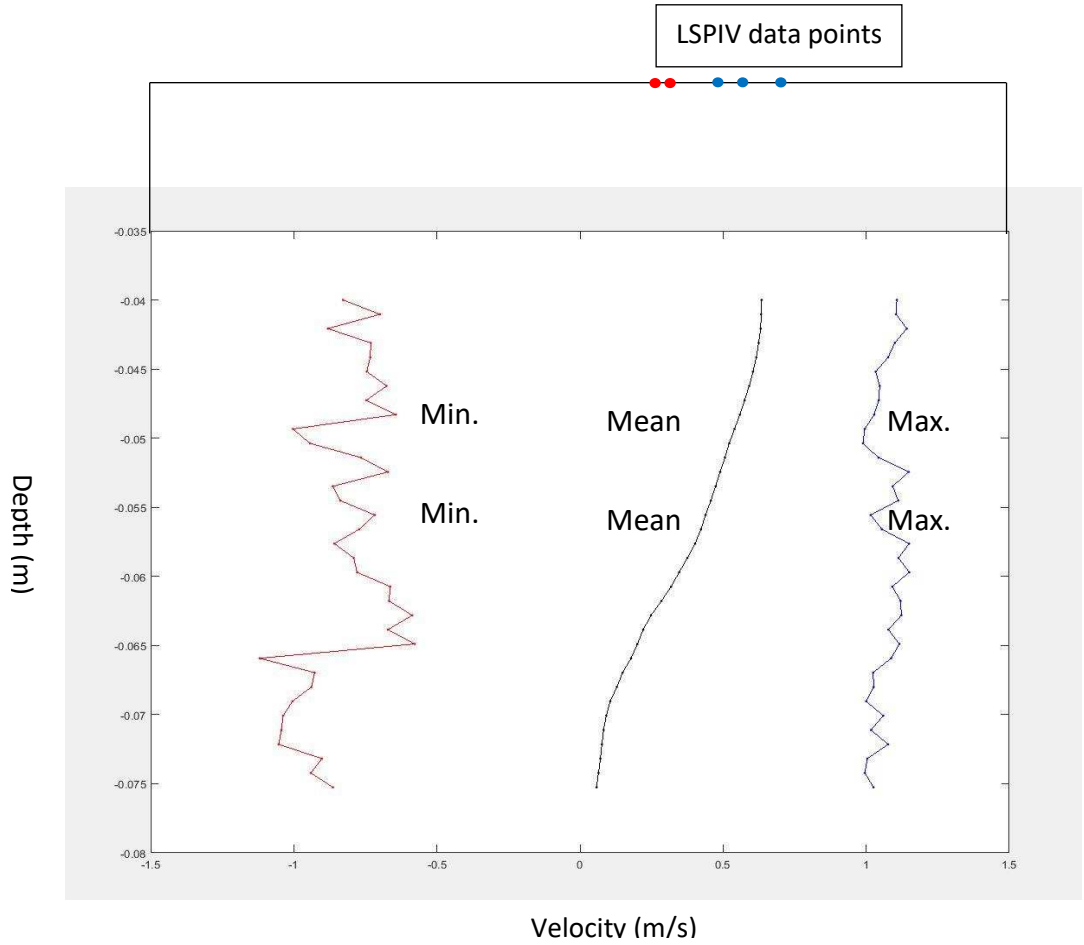

Figure 4.16: Maximum velocity (blue line), mean velocity (black line) and minimum velocity (red line) on the point (7.43, 0.63)

Table 4.4: LSPIV velocity data

	X	Y	VX	VY	VT
C-0.7	7.4832	0.6272	0.3884	-0.0656	0.393901
X-1	7.4328	0.6272	0.5281	-0.0119	0.528234
X-3	7.4328	0.6272	0.4951	-0.0234	0.495653
X-5	7.4776	0.6272	0.5773	-0.0308	0.578121
X-10	7.4328	0.6272	0.3421	-0.003	0.342113

Based on figure 4.16, can judge if the X-1, X-3 and X-5 three tests data are possible following the flow profile. But C-0.7 and X-10 tests have big error. It provides again that the tracer size from 3cm to 5cm is a better choice.

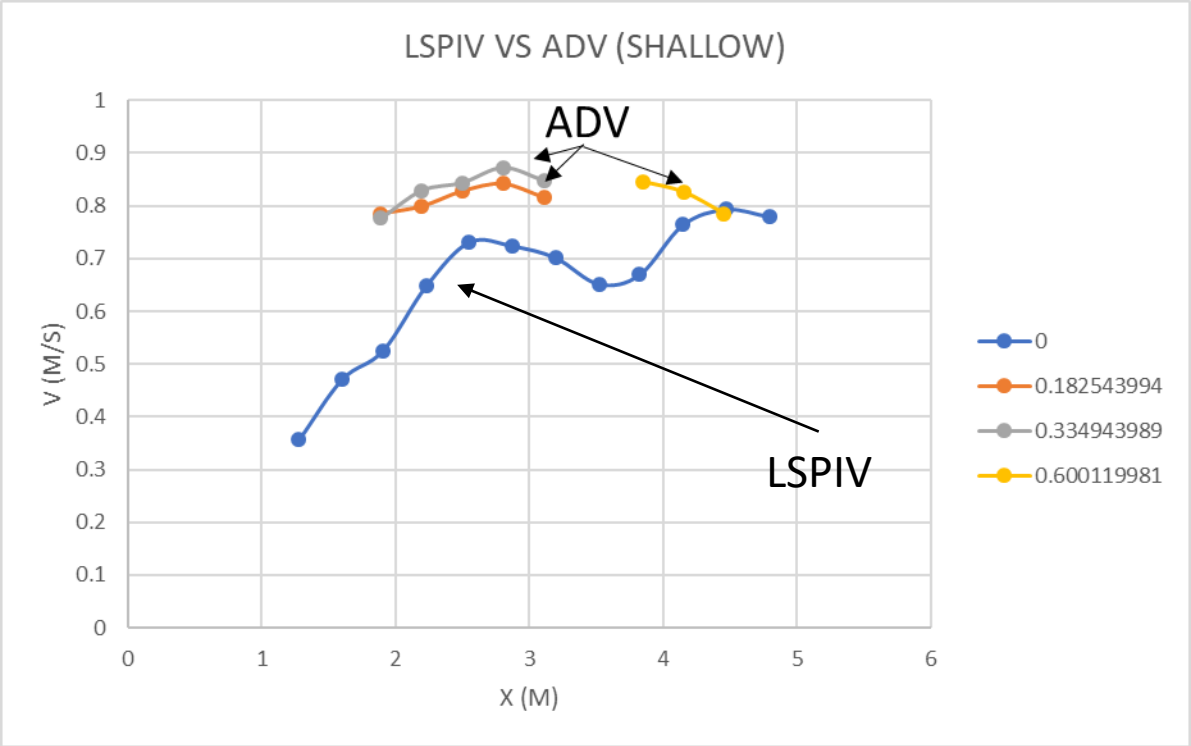

Figure 4.17: Velocity lines compare between the LSPIV method and ADV method for the shallow depth flow

And for the Tarbella flume channel test, the ADV velocity data provides the data reliability that is measured by LSPIV method. The different color means the different distance above the bed that was use ADV to measure the velocity. Figure 4.17 shows the velocity lines compare between the LSPIV method and ADV method on the shallow depth flow. It shows that the velocity hasa little significant difference because the depth of the flow is small. The flow profile makes a substantial change by the rocks and stones. And velocity in the flow is bigger than the surface velocity.

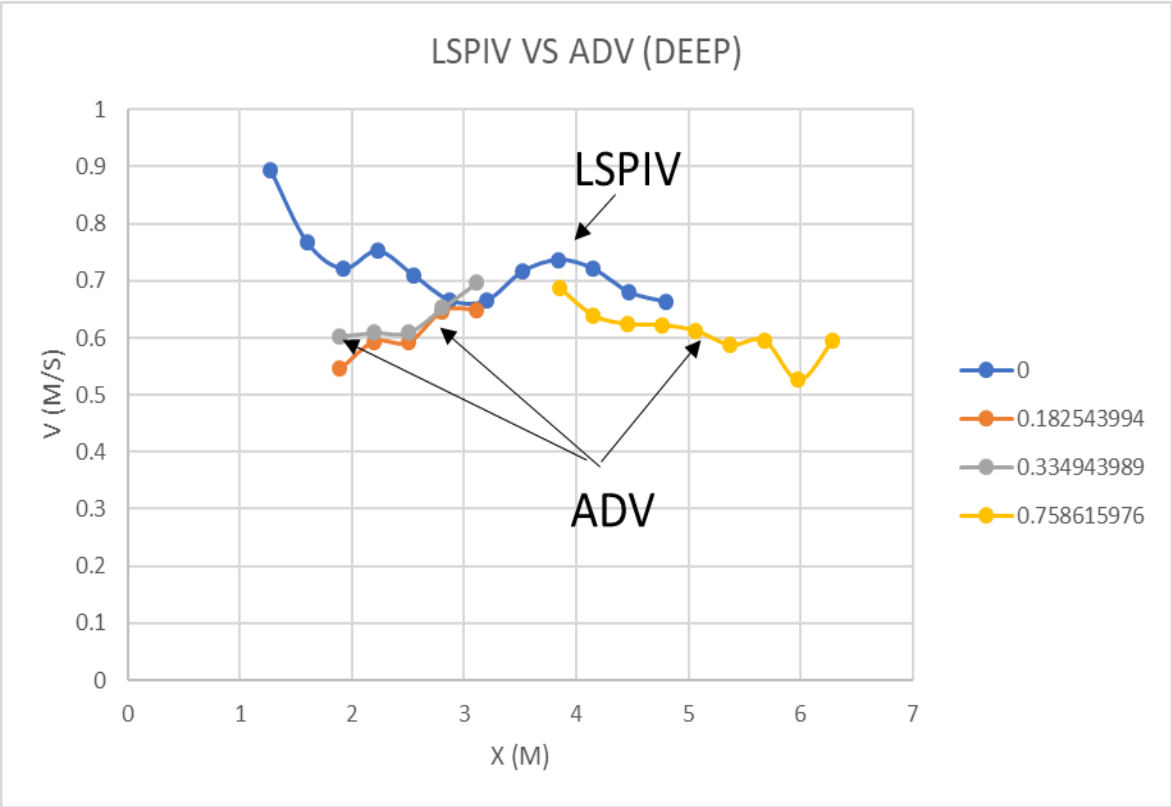

Figure 4.18: Velocity lines compare between the LSPIV method and ADV method for the deeper flow test

Figure 4.18 shows the velocity data from ADV compared with LSPIV data for the deep flow test. Also, the different color means the different distance above the bed that uses ADV to measure the velocity. The results are more similar in the flow length over last past after 4m. Also, the velocities also have a little difference from the 2m to 3m, if one considers the datum unevenness across the surface of the rocks and stones. The comparison indicates that the LSPIV-derived values of velocity compare favorably with velocity values obtained by means of the ADV measurements.

CHAPTER 5, CONCLUSIONS AND RECOMMENDATIONS

5.1 Introduction

The major objectives of this study were first to apply the Large Scale Particle Image Velocimetry (LSPIV) technique for use in Colorado State University's (CSU's) Hydraulics Laboratory, and then to determine how tracer size, using paper as tracers, influences LSPIV accuracy in measuring flow velocity. The study used two sets LSPIV measurements to calculate velocity fields of flows in two flume situations: a small flume and a large flume. In the course of meeting these objectives, it was important to provide guidance on how to apply LSPIV and on how to select appropriately sized tracer particles formed from paper, a convenient and readily available material. This thesis contains this guidance so as to help ensure convenient and accurate application of the LSPIV method in CSU's Hydraulics Laboratory. The present chapter states the main conclusions from the study and lists several recommendations regarding further use of the LSPIV technique.

5.2 Conclusions

The main conclusions resulting from the present study are as follow:

1. The LSPIV technique can be readily useable for many forms of future experiments conducted in CSU's Hydraulics Laboratory. Also, the procedure and software available of this technique make the technique useable for outdoor field work. Validation of LSPIV measurements is needed and can be readily done by relating velocity, measurements obtained using a stop-watch and ruler (measuring tracer drift) or with another instrument, such as an acoustic Doppler velocimeter;

2. The use of an effective size of tracer is a key factor that influences the accuracy of LSPIV measurements. For laboratory experiments, paper is a convenient and easily available material for forming a large number of tracers typically used for LSPIV measurements. However, the use of paper has limitations. If a paper tracer is too big or too small, inaccuracies can result. When too small, the paper can adhere together under the influence of surface tension. When the paper is too big, its movement is affected by velocities across too wide an area. The optimum size range was found to be about about 3.80% to 6.33% of the average width of the flow field;
3. When the tracer is placed in a flow field, it is important that surface- tension effects not cause the paper to bunch so as to form an excessively large tracer, which then adversely affects LSPIV measurement accuracy. In this respect, it is necessary that tracers be applied in a sufficiently dispersed manner so as not to overlap, and then that tracers do readily not come in contact so as to bunch and form an effectively larger tracer;
4. Adequate and reasonably uniform lighting are necessary for using the LSPIV technique. Light reflections off the water surface of a flow field can confuse the imaging software and reduce the visibility of tracers, thereby making the resulting velocity measurements of uncertain accuracy;
5. Application of the LSPIV technique requires selecting suitably sized interrogation areas (IA) and search areas (SA). The IA and SA areas are the areas within which tracer movement is interpreted into values of velocity. As a guideline, these areas should be 20 pixels for IA, and about 50 pixels for SA.

6. Also, important for the technique is the use of well-positioned benchmarks for use in the orthorectification step for determining local velocities. This step involves choosing clearly visible and obvious points to serve as benchmarks;
7. To ensure ample accuracy of velocity measurement, the video-camera must be positioned so as to minimize the need for orthorectification. Although the best angle of 90 degrees is not often possible, it is important to keep the video angle as close as possible to 90 degrees;
8. The video-camera should be fixed in position so as to eliminate camera vibration. Even a little vibration can adversely influence the image analysis and accuracy of velocity measurements;
9. Light reflection on a flow surface may adversely affect LSPIV interpretation of tracer movement. Figure 5.1 illustrates how light reflection can affect LSPIV interpretation of tracer movement; and,
10. Wind also will be a key factor that may adversely influence the LSPIV result, because wind drag may cause tracers to move in different directions that water currents. Also,

Figure 5.1: Influence of wind in rippling the water surface

wind can cause waves that alter the length of the flow path. So, if it is possible, make certain that the test environment does not have a major influence on a test. Figure 5.1, for example, shows the influence of wind on the surface of flow in the large flume.

5.3 Recommendations

LSPIV is an important technique for flow-field measurement, at least for flow fields on the surface of a flow. This technique likely will be extensively used for future experiments at CSU's Hydraulics Laboratory. Some recommendations regarding future use are listed below:

1. The Hydraulics Laboratory should keep aware of potential updates to the Fudaa-LSPIV software, which is presently the leading accessible software whose use is growing in extent of use. It should be anticipated that Fudaa-software updates will make the LSPIV technique easier and more efficient to use;
2. In the future, it is likely that the Fudaa-LSPIV software will add useful functions, such as the capacity to draw flow path-lines, label flow features of interest, and indicate hydraulics data of importance;
3. Whereas paper is a useful and inexpensive tracer material, the Hydraulics Laboratory should consider alternative tracer materials. A potential tracer material must be environmentally friendly, because it usually is lost when placed in a flow. Also, a tracer material should be easy to observe. Also, and ideally, tracer materials should not be subject to surface-tension effects when placed in water (i.e., tracers should not bunch together); and,
4. It should be anticipated that the LSPIV technique will be made useable for use involving drones (or remote-controlled small flying machines). This development will help the use of LSPIV is situations of field investigation.

5. Now LSPIV measurement only can be usedon the two-dimension condition. But real flow is three-dimension condition all. It will influence the result that make it inaccurate. In the future, maybe can be developed three-dimension condition LSPIV.

Generally, it should be anticipated that the LSPIV technique will become more accurate and easier to use. Ideally, people should be able to use LSPIV measurement any time and any place when they want to calculate velocities in a water-surface flow field.

REFERENCES

Aya, Shirou, Satoshi Kakinoki, Toshiaki Aburaya, and Ichiro Fujta. "Velocity and turbulence measurement of river flows by LSPIV." In Advances in Fluid Modeling & Turbulence Measurements: Proceedings of the 8th International Symposium on Flow Modeling and Turbulence Measurements: Tokyo, Japan, 4-6 December 2001, p. 177. World Scientific, 2002.

Basnet, Keshav, and R. Ettema. "A large-scale particle image velocimetry for resolving unsteady flow features at cylinders." In *Proceedings of the 34th World Congress of the International Association for Hydro-Environment Research and Engineering: 33rd Hydrology and Water Resources Symposium and 10th Conference on Hydraulics in Water Engineering*, p. 3378. Engineers Australia, 2011.

Creëlle, Stéphan, Rebeca Roldan, Anke Herremans, Dieter Meire, Kerst Buis, Patrick Meire, Tomas Van Oyen, Tom De Mulder, and Peter Troch. "Validation of large-scale particle image velocimetry to acquire free-surface flow fields in vegetated rivers." *Journal of Applied Water Engineering and Research* (2016): 1-12.

Zhang, Zhen, Lizhong Xu, and Huibin Wang. "Review of natural flow tracers for river surface imaging velocimetry." *Advances in Science and Technology of Water Resources* 34, no. 3 (2014): 81-88.

Fox, J. F., and A. Patrick. "Large-scale eddies measured with large scale particle image velocimetry." Flow measurement and Instrumentation 19, no. 5 (2008): 283-291.

Kantoush, Sameh A., Anton J. Schleiss, Tetsuya Sumi, and Mitsuhiro Murasaki. "LSPIV implementation for environmental flow in various laboratory and field cases." Journal of Hydro-environment Research 5, no. 4 (2011): 263-276.

Kim, Y., Marian Muste, Alexandre Hauet, Witold F. Krajewski, Anton Kruger, and Allen Bradley. "Stream discharge using mobile large-scale particle image velocimetry: A proof of concept." Water Resources Research 44, no. 9 (2008).

Kim, Y. (2006), Uncertainty analysis for non-intrusive measurement of river discharge using image velocimetry, Ph.D. thesis,Univ. of Iowa,Iowa City.

Li Yuzhu, and Jiang Chunbo. Engineering Fluid Mechanics: Volume. Tsinghua University Press, 2007.

Muste, Marian, I. Fujita, and A. Hauet. "Large-scale particle image velocimetry for measurements in riverine environments." Water Resources Research 44, no. 4 (2008).

Muste, M., Z. Xiong, and A. Kruger (1999), Error estimation in PIVapplied to large-scale flows, paper presented at 3rd International Workshop on Particle Image Velocimetry, Univ. of Calif., Santa Barbara, Calif., 16–18 Sept.

Peltier, Y., B. Dewals, P. Archambeau, M. Pirotton, and S. Erpicum. "Pressure and velocity on an ogee spillway crest operating at high head ratio: experimental measurements and validation."

Wilcox, David C. Basic Fluid Mechanics. 3rd ed. Mill Valley: DCW Industries, Inc., 2007. 664-668.